Chapter 3

Computer-Aided Drug Design Approaches to Study Key Therapeutic Targets in Alzheimer's Disease

Agostinho Lemos, Rita Melo, Irina S. Moreira, and M. Natália D.S. Cordeiro

Abstract

Alzheimer's Disease (AD) is one of the most common and complex age-related neurodegenerative disorders in elderly people. Currently there is no cure for AD, and available therapeutic alternatives only improve both cognitive and behavioral functions. For that reason, the search for anti-AD therapeutic agents with neuroprotective properties is highly demanding. Several research studies have implicated the involvement of G-Protein-Coupled Receptors (GPCRs) in diverse neurotransmitter systems that are dysregulated in AD, mainly in modulation of amyloidogenic processing of Amyloid Precursor Protein (APP) and of microtubule-associated protein *tau* phosphorylation and in learning and memory activities in in vivo AD models subjected to numerous behavioral procedures. In this chapter, a special focus will be given to the structure- and ligand-based in silico approaches and their applicability on the development of small molecules that target various GPCRs potentially involved in AD such as 5-hydroxytryptamine receptors, adenosine receptors, adrenergic receptors, chemokine receptors, histamine receptors, metabotropic glutamate receptors, muscarinic acetylcholine receptors, and opioid receptors.

Key words Alzheimer's disease, GPCRs, G-proteins, Drug design, Docking, Pharmacophore, QSAR

1 Introduction

Alzheimer's disease (AD) is a neurodegenerative disorder clinically characterized by a progressive and irreversible loss of memory and impairment of other cognitive functions, which ultimately results in a complete degradation of intellectual and mental activities. Although age represents a critical risk factor, a combination of genetic, lifestyle, and environmental factors may contribute for the development of AD. Being the most common cause of dementia in elderly people, continuous research efforts have been devoted to unravel the etiology of AD with the objective of developing effective pharmacological treatments.

Although the underlying mechanism of AD is not yet well understood, several neuropathological hallmarks are thought to be

Kunal Roy (ed.), *Computational Modeling of Drugs Against Alzheimer's Disease*, Neuromethods, vol. 132, DOI 10.1007/978-1-4939-7404-7_3, © Springer Science+Business Media LLC 2018

involved in the neurodegeneration in AD, including (i) deficiency on cholinergic transmission in the Central Nervous System (CNS) due to an extensive loss of cholinergic neurons which results in a deficit of AcetylCholine (ACh) in specific regions of the brain (cholinergic hypothesis) (reviewed in [1, 2]); (ii) abnormal clustering of neurotoxic β-amyloid (Aβ) fragments and formation of senile plaques that occur as a consequence of an imbalance between the amyloidogenic (mediated by β- and γ-secretases) and non-amyloidogenic (mediated by α- and γ-secretases) processing pathways of Amyloid Precursor Protein (APP) and an inefficient clearance of Aβ oligomers (amyloid hypothesis) (reviewed in [3, 4]); and (iii) hyperphosphorylation of Serine (Ser), Threonine (Thr), and Tyrosine (Tyr) sites in microtubule-associated *tau* proteins that leads to the destabilization of neuronal microtubules, the formation of *tau* aggregates and NeuroFibrillary Tangles (NFT), and the collapse of neuronal signaling (*tau* hypothesis) (reviewed in [5, 6]). With the increasing number of people suffering from age-related neurodegenerative disorders, particularly AD, effective therapeutic alternatives are highly demanding. Currently, pharmacological research has been focused on the discovery of drug candidates with neuroprotective properties, which target disease-modifying effects, contributing to the blockade of neuronal apoptosis and subsequent disease progression. These strategies are based on targeting key proteins involved in amyloidogenic processing of APP (activation of α-secretase, inhibition of β- and γ-secretases, prevention of Aβ aggregation, and promotion of Aβ clearance) and in *tau* pathology (inhibition of *tau*-phosphorylating kinases, prevention of *tau* aggregation, and promotion of *tau* aggregate disassembly). However, current clinically available AD therapies are essentially symptomatic and target mainly AcetylCholinEsterase (AChE) (donepezil, rivastigmine, and galantamine) and *N*-methyl-D-aspartate receptor (memantine), which lead to the reversion of dysfunctions on cholinergic and glutamatergic neurotransmission, respectively. Moreover, neurodegeneration is not restricted to a particular neurotransmitter system. Histaminergic, adenosinergic, adrenergic, and serotonergic, among other neurotransmitter systems, are also dysregulated in AD. Interestingly, numerous studies have implicated the role of G-Protein-Coupled Receptors (GPCRs) in the pathogenesis of AD, particularly in the modulation of the distinct therapeutic targets involved in amyloidogenic processing of APP and in microtubule-associated *tau* protein aggregation, and the influence of GPCR modulators in AD animal models subjected to various learning and memory paradigms. Potential GPCR-derived therapeutic targets for AD include 5-HydroxyTryptamine 2A, 2C, 4, and 6 Receptors (5-HT_{2A}R [7, 8], 5-HT_{2C}R [7, 9], 5-HT_4R [10, 11, 12, 13], and 5-HT_6R [14, 15, 16, 17]); Adenosine A_1 and A_{2A} Receptors (A_1AR [18, 19, 20] and A_{2A}AR [18, 21, 22, 23, 24]); α_{2A}- and β_2-Adrenergic Receptors (α_{2A}-AR [25] and β_2-AR [26, 27, 28]); CC motif chemokine

receptor 2 (CCR_2 [29, 30]); CXC motif chemokine receptor 2 ($CXCR_2$ [31, 32, 33]); corticotropin-releasing factor receptor 1 ($CRFR_1$ [34, 35, 36, 37]); δ-opioid receptors (DOR [38]); histamine H_3 receptor (H_3R [39, 40, 41]); metabotropic glutamate receptor types 1, 2, and 5 ($mGluR_1$ [42, 43, 44, 45], $mGluR_2$ [42, 46, 47], and $mGluR_5$ [42, 48, 49]); and M_1, M_2, and M_3 muscarinic acetylcholine receptors (M_1 mAChR [50, 51, 52, 53, 54], M_2 mAChR [54, 55], and M_3 mAChR [53, 54]), among others. In this chapter, we will provide an overview of the structure-based and ligand-based computational approaches widely employed in in silico medicinal chemistry to target the mentioned GPCRs potentially implicated in AD.

2 GPCRs: A Case Study of Potential Targets for AD

Being one of the most heavily investigated drug targets in the pharmaceutical industry, GPCR-targeting drugs represent about ~30–40% of the current market for human therapeutics and have been subjected to a considerable number of computational studies [56, 57]. They comprise a large family of membrane-embedded proteins that mediate important physiological functions through interaction with various endogenous ligands, including ions, proteins, peptides, amines, hormones, chemokines, and neurotransmitters [58, 59]. Structurally, a single polypeptide chain with a variable length that crosses the phospholipidic bilayer seven times adopting the typical structure of seven transmembrane (TM) α-helices connected to extracellular (ECL) and intracellular (ICL) loops characterizes the receptors belonging to this family [60]. Based on sequence homology and phylogenetic analysis, human GPCRs can be classified into five main families of receptors: *glutamate* (Class C, 22 members), *rhodopsin* (Class A, 672 members), *adhesion* (33 members), *frizzled/Taste2* (Class F, 36 members), and *secretin* (Class B, 15 members), which are usually shortened to the acronym *GRAFS* [60]. The complexity of GPCR-induced signaling is determined by their association with specific heterotrimeric guanine nucleotide-binding proteins (G-proteins) within the plasma membrane. Heterotrimeric G-proteins are composed of a guanine-binding α-subunit (G_α) and a dimer consisting of the β- and γ-subunits ($G_{\beta\gamma}$). In their inactive state, G_α is bound to guanosine diphosphate (GDP) and associated with $G_{\beta\gamma}$. In the extracellular site, the binding of an agonist stabilizes the active conformation of the receptor, which couples to heterotrimeric G-proteins, leading to GDP release and guanosine triphosphate (GTP) binding to the G_α subunit. Subsequently, the GTP binding induces a conformational switch on the G_α subunit, which promotes the release of G-proteins

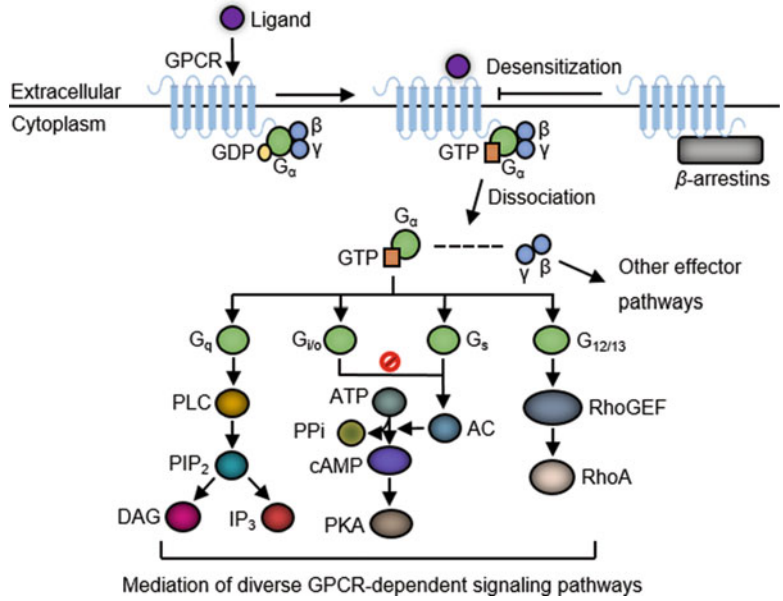

Fig. 1 General diagram of GPCR signaling mediated by activation of G_{α} subunit of heterotrimeric G-proteins. *AC* Adenylyl Cyclase, *ATP* Adenosine TriPhosphate, *cAMP* cyclic Adenosine MonoPhosphate, *DAG* DiAcylGlycerol, *GDP* Guanosine DiPhosphate, *GTP* Guanosine TriPhosphate, *IP_3* Inositol 1,4,5-trisPhosphate, *PIP_2* PhosphatidylInositol 4,5-bisPhosphate, *PKA* Protein Kinase A, *PLC* PhosphoLipase C, *PPi* inorganic PyroPhosphate, *RhoA* Ras homolog gene family, member A, *RhoGEF* Rho Guanine nucleotide Exchange Factor

from GPCR and the dissociation of heterotrimeric G-proteins into G_{α} and $G_{\beta\gamma}$ subunits [61, 62]. The G_{α} ($G_{\alpha s}$, $G_{\alpha i/o}$, $G_{\alpha q}$, $G_{\alpha 12/13}$) and $G_{\beta\gamma}$ subunits amplify and propagate their transduction signals by modulating the activity of distinct downstream cellular effectors, including adenylyl and guanylyl cyclases, phospholipases, phosphodiesterases, and phosphoinositide 3-kinases, that in turn induces an increasing or decreasing production of second messengers, such as Ca^{2+}, diAcylglycerol (DAG), inositol 1,4,5-trisphosphate (IP_3), cyclic adenosine monophosphate (cAMP), and cyclic guanosine monophosphate (cGMP) that triggers a wide range of cellular responses [63, 64] (Fig. 1).

Nevertheless, not all GPCR-dependent signaling pathways are mediated via heterotrimeric G-proteins. The persistent stimulation of a specific agonist may contribute to a decreasing responsiveness of GPCRs, eliciting a process of receptor desensitization, which terminates or attenuates the receptor signaling. Two families of regulatory proteins participate in the mechanism of GPCR desensitization, including second messenger-dependent protein kinases and G-protein-coupled receptor kinases (GRKs). Second messenger-dependent protein kinases, protein kinases A (PKA) and C (PKC), induce a conformational change in the receptor

through GPCR phosphorylation, directly uncoupling GPCR to heterotrimeric G-proteins. This mechanism of receptor regulation can be mediated in the absence of GPCR occupancy by an agonist through a process of heterologous desensitization. In contrast, GPCR occupancy is required for the recruitment of GRKs on receptor desensitization (homologous desensitization). The GRKs preferentially induce the phosphorylation in an agonist-bound conformation, leading to a significant attenuation of receptor signaling [65]. GRK-dependent phosphorylation enables GPCRs to interact with high affinity to a class of multifunctional scaffold proteins called β-arrestins, which sterically blocks further interactions between the G-protein and the activated receptor, preventing GPCR signaling [66]. Additionally, receptor-bound β-arrestins can also promote different signaling pathways or act as adapter proteins, promoting receptor sequestration through interaction with components of the cellular machinery required for clathrin-mediated endocytosis [67]. This mechanism is critical not only for receptor signaling desensitization but also for receptor resensitization for a next round of GPCR activation. Other mechanisms of desensitization include the receptor proteolysis in lysosomes [68], dynamic regulation of receptor gene expression [69], and GTP hydrolysis by regulators of G-protein signaling (RGS) proteins [70, 71].

3 In Silico Approaches in the Discovery of New Modulators of GPCR-Derived Therapeutic Targets for AD

A wide array of Computer-Aided Drug Design (CADD) methodologies have been employed as a complementary tool to the high-throughput screening (HTS) approaches to identify new GPCR modulators with therapeutic potential for AD. One critical stage in in silico drug design of GPCR modulators is the discovery of novel lead compounds (or hit-to-lead optimization), which can be accomplished using different strategies such as virtual screening of large libraries of chemical compounds using structure-based or ligand-based drug design approaches (Fig. 2).

3.1 Structure-Based Drug Design Approaches

Over the last years, the progress of the structural biology on determination of accurate three-dimensional (3D) structures of GPCRs has furnished a valuable tool for drug design of GPCR modulators by structure-based drug design approaches, such as homology modeling, virtual screening, and fragment screening. In fact, X-ray crystallography and Nuclear Magnetic Resonance (NMR) studies provide detailed and atomic-level information of GPCR-drug interactions. As their function implicates, GPCRs are membrane-bound proteins, which make experimental 3D structure elucidation, by X-ray crystallography or NMR studies, an extremely

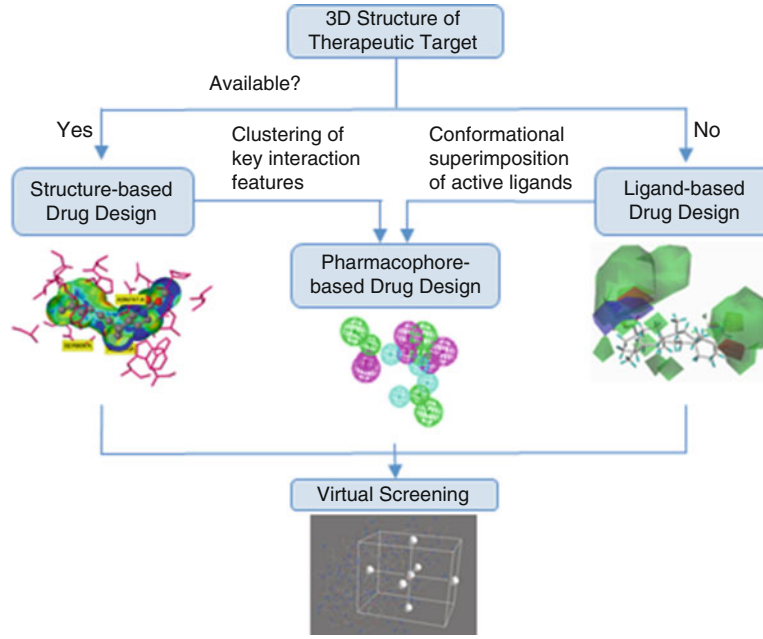

Fig. 2 General diagram of in silico drug design approaches based on the availability of 3D structural information of therapeutic targets (Representative images were extracted from [72, 73])

complex and challenging task compared to globular proteins (reviewed in [74]). Until the elucidation of the X-ray diffraction structure at 2.8 Å resolution of Class A GPCR bovine rhodopsin in 2000 [75], no X-ray structures of any GPCR were available. The high quality and detailed structure of bovine rhodopsin provided a huge progress of understanding of GPCRs at molecular level and paved the way for structure-based design approaches for GPCRs. Rhodopsin was chosen as the typical example for structural studies due to the fact that it is easy to obtain considerable quantities of functional protein with high stability under conditions that denature other GPCRs [76]. For many years, the structure of inactive state of rhodopsin provided the only template sequence for molecular modeling studies in homologous GPCRs (reviewed in [77]), which was a limitation for the study of other GPCR family members. Although rhodopsin-like or Class A GPCRs present similar structural features with the prototypical bovine rhodopsin, especially concerning the TM domain, they share a low overall homology. Moreover, other GPCRs belonging to *glutamate*, *adhesion*, *secretin*, and *frizzled/taste2* families have no homology with *rhodopsin*. Also, the distinct ligand binding and mechanism of activation of rhodopsin from other GPCRs make the understanding from rhodopsin structure how such a diverse plethora of ligands could activate the large family of GPCRs difficult. Additionally, X-ray

structure of rhodopsin represents the inactive form of the receptor, while the active form would be much more suitable for rational drug design. The experimental progress in obtaining crystal GPCR structures was very slow. In fact, it took more than seven years until the 3D structures of β_2-AR complexed with carazolol [78, 79] and turkey β_1-AR complexed with cyanopindolol [80] were solved. With the development of receptor crystallization techniques, a number of technical issues derived from the low expression of GPCRs and their structural instability have been overcome, thereby resulting in an accelerated increase in solved GPCR structures. Currently, there are more than 150 3D structures of apo-, peptide-, natural ligand-, agonist-, and antagonist-bound GPCR complexes available within Protein Data Bank (PDB), in which the family A GPCR structures have been the most frequently reported ones. Only two family B, two family C, and one frizzled 3D GPCR structures have been published. Given the diverse physiological and pathological implications of their signaling, particularly in AD and other neurodegenerative disorders, GPCRs have been considered very promising therapeutic targets for pharmaceutical applications. Moreover, the identification of 3D GPCR structures provides a wealth of information to pharmaceutical researchers for drug design of GPCR modulators with neuroprotective properties for the treatment of AD.

Drug discovery efforts targeting GPCRs have been mainly focused on the development of ligands which interact with the orthosteric binding site for endogenous ligands, but a wide variety of GPCRs possess additional topographically distinct druggable sites (allosteric sites) (reviewed in [81, 82]). This allows the pharmacological modulation of particular GPCRs not only by conventional orthosteric agonists or antagonists but also by positive allosteric modulators (PAMs) or negative allosteric modulators (NAMs) with potentially high receptor subtype selectivity that either increase or reduce the receptor responsiveness, respectively (reviewed in [81, 82]). Since GPCRs interact with a plethora of intracellular signaling proteins, such as heterotrimeric G-proteins and β-arrestins, and modulate distinct intracellular pathways, distinct GPCR-targeted ligands are expected to stabilize various structural conformations and signaling states of GPCRs. In fact, specific GPCR-targeted ligands possess the ability to selectively evoke a particular stimulus-response, which results in a unique ligand-dependent signaling profile referred to as functional selectivity, biased signaling, or stimulus bias. The functional selectivity phenomenon has been explored in medicinal chemistry for the design of GPCR-targeted drugs with pathway selectivity (reviewed in [83, 84]).

In order to address how drug-dependent GPCR signaling relates to the concept of functional selectivity, atomistic-level information about the mode of ligand-GPCR interactions coupled with

its two signaling partners, G-proteins and β-arrestins, is required [85]. However, relevant structure-function information is still scarce. The first X-ray crystal structure of a GPCR/G-protein complex only became available in 2011, in which the β_2-AR was complexed to $G_{\alpha s}$ protein [86]. Given the limitations of the crystallizable fragments and the static nature of this single available model, this important but restricted information is insufficient to understand the function of such a complex biological system. Nowadays, molecular dynamics (MD) simulations are a treasured resource for the study of GPCRs and can be applied to better understand their function. In fact, the usage of MD simulations has been extremely relevant to model the process of GPCR activation on an atomistic level [87, 88], to study ligand recognition or GPCR oligomerization [89] by generating ensembles of energetically accessible conformations [90, 91]. The overall construction of the membrane-protein systems is harder than for soluble proteins, but a few tools provide accurate and fast alternatives to step-by-step manual construction, such as Chemistry at HARvard Macromolecular Mechanics-Graphical User Interface (CHARMM-GUI) [92, 93], QwikMD [94], and high-throughput molecular dynamics (HTMD) [95]. The membrane environment can be explicitly (all atom) or implicitly (coarse grained (CG)) modeled. However, when a researcher aims to fully characterize the ligand-GPCR interactions, the explicit option should be chosen as it allows a detailed characterization of pairwise interactions and the measurement of a variety of chemical-physical features. While the dynamics of activation are beginning to be clarified for individual GPCRs, an increasingly important consideration pertains to the identity of the "signaling unit." Thus, for many years, the GPCRs were thought to function only as monomers, but increasing evidence suggests that they can form homodimers, heterodimers, or higher-order oligomers. It was already demonstrated that minimal functional signaling unit is a complex between a GPCR and heterotrimeric G proteins [56]. Various dimer interfaces have been proposed, but a rearrangement of the dimerization interface to form a TM4-TM4 interface is likely a critical component of activation [96]. Nonetheless, the mechanistic and structural details of the ligand-GPCR function are not known, either at the level of the receptor signaling unit or with regard to the functional epitope between GPCR/G-proteins and GPCR/β-arrestins. These aims could be also achieved upon long all-atom MD simulations of the complete systems and their subsequent analysis.

Another in silico approach widely employed in drug design is docking-based virtual screening, which consists of a wide range of computational methodologies that analyze the interaction of large databases of small-molecule drug candidates against a 3D representation of the structure of a therapeutic target protein of interest (reviewed in [97]). This approach is usually performed through

molecular docking, in which each "virtual" drug candidate is docked into the X-ray crystallographic structure of the therapeutic target or, if 3D structure is not available, into a model of the target (homology model-based virtual screening), using algorithms that explore the multiple binding conformations of the ligand inside the binding cavity of a target protein. Subsequently, for each of the generated ligand conformation, the strength of their binding affinity to the target is predicted through the determination of a scoring function. In most of the automated molecular docking studies, a flexible ligand is docked in a rigid protein, since a flexible macromolecular target would demand a high cost of computational time (reviewed in [97]). Docking-based virtual screening can be applied to databases of commercially available compounds and *in-house* ligands that have been previously synthesized and tested in vitro or databases of virtual ligands that can be synthesized according to their calculated docking scores. Moreover, docking-based virtual screening may be also useful following in vitro studies for the interpretation of potential target-ligand interactions. Therefore, the main purpose of structure-based virtual screening is to select the ligand structures that are most likely to bind to a certain therapeutic target of interest, providing a library of the best scored ligands for experimental screening and, thereby, improving the overall efficacy of the drug screening process. Currently, there are a number of in silico tools widely employed in protein-ligand docking studies including automated docking (AutoDock) [98], AutoDock Vina [99], CHARMm-based DOCKER (CDOCKER) [100], FlexX [101], Genetic Optimization of Ligand Docking (GOLD) [102], Grid-based Ligand Docking with Energetics (GLIDE) [103], Internal Coordinate Mechanics (ICM) [104], molecular Interaction FingerPrints (IFP) [105], Induced-Fit Docking (IFD) [106], Library Docking (LibDock) [107], MolGridCal [108], and Protein-Ligand ANT System (PLANTS) [109], among others. Table 1 summarizes the most relevant structure-based studies performed by these docking programs for the GPCRs involved in AD.

3.2 Ligand-Based Drug Design Approaches

The GPCR ligand-based drug design useful for the identification of therapeutic agents for AD relies on knowledge of compounds that are recognized to modulate the activity of this family of TM proteins and represents a suitable in silico approach when the structural information of the therapeutic target is not available. In fact, the majority of potential drug candidates that act on GPCRs have been conceived from ligand-based methodologies, due to the restricted availability of 3D structural data on GPCRs. Various ligand-based drug design approaches have been used to better understand the mechanism of action of GPCR modulators and to screen for new bioactive molecules. Table 2 reports the applicability of ligand-based drug design approaches on the discovery of GPCR modulators with therapeutic potential for AD using large databases of

Table 1
Structure-based drug design techniques for the modulation of potential GPCR-derived therapeutic targets of AD

GPCR: Adenosine A_1 receptor (A_1AR)		
Ligands		
Adenosine		
Drug design technique(s)	**Computational tool(s)**	**References**
Docking into a human A_1AR model using the X-ray structure of bovine rhodopsin as template (PDBid 1F88)	AUTODOCK	[110]
Ligands		
Library of commercially available compounds (ZINC database) with molecular weight between 250 and 350 g/mol, less than 7 rotatable bonds, and a xlogP between 2.5 and 3.5		
Drug design technique(s)	**Computational tool(s)**	**References**
Docking into a human A_1AR model using the X-ray structure of $A_{2A}AR$ as template (PDBid 3EML)	DOCK	[111]
Ligands		
DPCPX, 52 active antagonists, and 1000 decoys		
Drug design technique(s)	**Computational tool(s)**	**References**
Docking into 12 models of A_1AR using the X-ray structure of $A_{2A}AR$ as template (PDBid 3EML)	DOCK, VINA, GOLD	[112]
GPCR: Adenosine A_{2A} receptor ($A_{2A}AR$)		
Ligands		
Library of 545,000 CNS drug-like compounds		
Drug design technique(s)	**Computational tool(s)**	**References**
Docking into a $A_{2A}AR$ model using the X-ray structure of turkey β_1-AR as template (PDBid 2VT4)	GLIDE	[113]
Ligands		
Library of 4,300,000 drug-like compounds		
Drug design technique(s)	**Computational tool(s)**	**References**
Docking into X-ray structure of $A_{2A}AR$ (PDBid 3EML)	ICM	[114]
Ligands		
ZM241385		

(continued)

Table 1
(continued)

Drug design technique(s)	Computational tool(s)	References
Docking into X-ray structure of $A_{2A}AR$ (PDBid 3EML) and into a $A_{2A}AR$ model using X-ray structure of β_2-AR as template (PDBid 2R4R)	GLIDE XP, InducedFit, MOE Tabu search	[115]
Ligands		
Library of commercially available compounds (ZINC database)		
Drug design technique(s)	**Computational tool(s)**	**References**
Docking into four X-ray structures of $A_{2A}AR$ (PDBid 3QAK; PDBid 2YDO; PDBid 2YDV; PDBid 3EML)	DOCK	[116]
Ligands		
Library of commercially available compounds (ZINC database) with molecular weight less than 350 g/mol, less than seven rotatable bonds, and logP lower than 3.5		
Drug design technique(s)	**Computational tool(s)**	**References**
Docking into X-ray structure of $A_{2A}AR$ (PDBid 3EML)	DOCK	[117]
GPCR: α_{2A}-Adrenergic Receptor (α_{2A}-AR)		
Ligands		
Library of WOMBAT 2007.1 compounds		
Drug design technique(s)	**Computational tool(s)**	**References**
Docking into a α_{2A}-AR model using the X-ray structure of human β_2-AR as template (PDBid 2RH1)	GLIDE	[118]
Ligands		
Chlorpromazine, spiperone, spiroxatrine, quinazolines, dopamine, adrenaline, clonidine, dexmedetomidine, BRL-44408, JP-1302, OPC-2836, ARC239, clozapine, WB4101		
Drug design technique(s)	**Computational tool(s)**	**References**
Docking into a α_{2A}-AR model using the X-ray structure of human dopamine D_3 receptor (D_3R) as template (PDBid 3PBL) as template	GLIDE	[119]
GPCR: β_2-Adrenergic receptor (β_2-AR)		
Ligands		
Library of commercially available compounds (ZINC database)		
Drug design technique(s)	**Computational tool(s)**	**References**
Docking into the X-ray structures of β_2-AR (PDBid 2RH1; PDBid 3P0G) and virtual screening	PLANTS, IFP	[120]

(continued)

Table 1
(continued)

Ligands		
Library of commercially available compounds (ZINC database)		
Drug design technique(s)	**Computational tool(s)**	**References**
Docking into the X-ray structure of β_2-AR (PDBid 2RH1)	DOCK	[121]
Ligands		
Library of commercially available compounds (ZINC database)		
Drug design technique(s)	**Computational tool(s)**	**References**
Docking intothe X-ray structure of β_2-AR (PDBid 3SN6)	MolGridCal, AUTODOCK VINA, LibDock, CDOCKER, Discovery Studio 2.5, NAMD	[108]
GPCR: CC motif chemokine receptor 2 (CCR_2)		
Ligands		
Teijin, RS-504393, 2-amino-*N*-(2-(((1*S*,2*R*)-2-((4-(methylthio)benzyl)amino)cyclohexyl)amino)-2-oxoethyl)-5-(trifluoromethyl)benzamide, 2-amino-*N*-(2-(((3*S*,4*R*)-4-((4-(methylthio)benzyl)amino)piperidin-3-yl)amino)-2-oxoethyl)-5-(trifluoromethyl)benzamide		
Drug design technique(s)	**Computational tool(s)**	**References**
Docking into a CCR_2 model using the X-ray structure of CXC chemokine receptor 4 ($CXCR_4$) as template (PDBid 3ODU)	GROMACS, AUTODOCK	[122]
Ligands		
TAK779, Teijin-comp1, JnJ-comp1, Merck-comp55, INCB3344, and BMS-comp22		
Drug design technique(s)	**Computational tool(s)**	**References**
Docking into a CCR_2 model using the X-ray structure of $CXCR_4$ as template (PDBid 3ODU)	AMBER, GLIDE	[123]
GPCR: Corticotropin-releasing factor receptor 1 ($CRFR_1$)		
Ligands		
Dihydropyrrole[2,3-*d*]pyridines		
Drug design technique(s)	**Computational tool(s)**	**References**
Docking into a $CRFR_1$ model using the X-ray structure of glucagon and calcitonin receptors as templates	MacroModel/BatchMin	[124]
GPCR: δ-Opioid receptor (DOR)		
Ligands		
NTB, NTI, NTIR, BNTX, SNC80, SNC67, BW373U86, SIOM, TAN-67, SB219825, SB206848, SUPERFIT, *cis*-(+)-3-methylfentanyl		

(continued)

Table 1
(continued)

Drug design technique(s)	**Computational tool(s)**	**References**
Docking into three DOR models using the X-ray structure of bovine rhodopsin as template (PDBid 1F88)	AUTODOCK	[125]
Ligands		
Morphine		
Drug design technique(s)	**Computational tool(s)**	**References**
Docking into a DOR model using the X-ray structure of bovine rhodopsin (PDBid 1F88) and the theoretical model of bovine rhodopsin based on electron microscopy (PDBid 1B0J) as templates	MOE	[126]
GPCR: Histamine H_3 receptor (H_3R)		
Ligands		
Library of compounds derived from ChEMBL database and VU-MedChem fragment library		
Drug design technique(s)	**Computational tool(s)**	**References**
Virtual fragment screening into a H_3R model using the X-ray structure of histamine H_1 receptor (H_1R) as template (PDBid 3RZE)	PLANTS, GOLD	[127]
Ligands		
Library of 418 H_3R antagonists		
Drug design technique(s)	**Computational tool(s)**	**References**
Docking into a H_3R model using the X-ray structure of bivine rhodopsin (PDBid 1HZX) as template	GOLD	[128]
Ligands		
Library of non-imidazole H_3R antagonists		
Drug design technique(s)	**Computational tool(s)**	**References**
Docking into a H_3R model using the X-ray structure of bovine rhodopsin as template (PDBid 1L9H)	GOLD	[129]
GPCR: Metabotropic glutamate receptor type 1 ($mGluR_1$)		
Ligands		
L-Glu, QUIS, Ibo, (1*S*,3*R*)-ACPD, *S*-4CPG, *S*-4C3HPG, *S*-4H3CPG, M4CPG, *S*-3HPG, UPF523		
Drug design technique(s)	**Computational tool(s)**	**References**
Docking into a NH_2-terminal domain of $mGluR_1$ model using the X-ray structures of leucine/isoleucine/valine-binding protein	SYBYL	[130]

(continued)

Table 1
(continued)

(LIVBP) (PDBid 2LIV) and of leucine-binding protein (LBP) (PDBid 2LBP) as templates		
GPCR: M_1 muscarinic AcetylCholine Receptor (M_1 mAChR)		
Ligands		
L005771, L005772, L005773, L006454, L014151, pilocarpine, NCC11-1314, NCC11-1585, NCC11-1607, nebracetam, oxotremorine, oxotremorine-M, quinuclidine, RU47213, SDZ ENS 163, pilofrin, gliatilin (TN), sabcomeline, VU0357017, xanomeline, pentylthio-TZTP		
Drug design technique(s)	**Computational tool(s)**	**References**
Docking into a M_1 mAChR model using the X-ray structure of M_3 mAChR as template (PDBid 4DAJ)	GLIDE	[131]
Ligands		
Flavonoids		
Drug design technique(s)	**Computational tool(s)**	**References**
Docking into a M_1 mAChR model using the X-ray structure of M_3 mAChR as template (PDBid 4DAJ)	GLIDE, AUTODOCK	[132]
GPCR: M_2 muscarinic AcetylCholine Receptor (M_2 mAChR)		
Ligands		
Library of lead-like compounds and fragments derived from the ZINC database		
Drug design technique(s)	**Computational tool(s)**	**References**
Docking into the X-ray structure of M_2 mAChR (PDBid 3UON) and virtual screening	DOCK	[133]
GPCR: M_3 muscarinic AcetylCholine Receptor (M_3 mAChR)		
Ligands		
Library of lead-like compounds and fragments derived from the ZINC database		
Drug design technique(s)	**Computational tool(s)**	**References**
Docking into the X-ray structure of M_3 mAChR (PDBid 4DAJ) and virtual screening	DOCK	[133]
GPCR: 5-HydroxyTryptamine 2A Receptor (5-HT_{2A}R)		
Ligands		
Library of 5-HT_{2A}R agonists (serotonin, DOI, mescaline, LSD, 5-MeO-alpha-ET, psilocin, bufotenine, dimethyltryptamine) and antagonists (nefazodone, aripiprazole, haloperidol, cyproheptadine, trazodone, clozapine, ketanserin, spiperone, risperidone)		

(continued)

Table 1
(continued)

Drug design technique(s)	Computational tool(s)	References
Docking into human 5-HT_{2A}R model using the X-ray structure of β_2-AR (PDBid 3SN6) as template and virtual screening	GLIDE	[134]
Ligands		
Serotonin, dopamine, DOI, LSD, haloperidol, ketanserin, clozapine, risperidone		
Drug design technique(s)	**Computational tool(s)**	**References**
Docking into human 5-HT_{2A}R model using the X-ray structure of β_2-AR (PDBid 2RH1) as template	AUTODOCK	[135]
Ligands		
(Aminoalkyl)benzo and heterocycloalkanones		
Drug design technique(s)	**Computational tool(s)**	**References**
Docking into the transmembrane α-helices bundle of 5-HT_{2A}R model using the X-ray structure of bovine rhodopsin (PDBid 1F88) as template	AMBER	[136]
GPCR: 5-HydroxyTryptamine 2C Receptor (5-HT_{2C}R)		
Ligands		
(Aminoalkyl)benzo and heterocycloalkanones		
Drug design technique(s)	**Computational tool(s)**	**References**
Docking into the transmembrane α-helices bundle of 5-HT_{2C}R model using the X-ray structure of bovine rhodopsin (PDBid 1F88) as template	AMBER	[136]
Ligands		
11-Chloro-2,3,4,5-tetrahydro-1*H*-[1, 4]diazepino[1,7-*a*]índole, 8,9-dichloro-2,3,4,4*a*-tetrahydro-1*H*-pyrazino[1,2-*a*]quinoxalin-5(6*H*)-one, (*S*)-1-(2-aminopropyl)-7-fluoro-1*H*-indazol-6-ol, (*R*)-1-(7-(2-chlorophenyl)-5-fluoro-2,3-dihydrobenzofuran-2-yl)-*N*-methylmethanamine, *N*-(3-(4-methylimidazolidin-1-yl)phenyl)-5,6-dihydrobenzo[*h*]quinazolin-4-amine, *N*-(4-methoxy-3-(4-methylpiperazin-1-yl)phenyl)-1,2-dihydro-3*H*-benzo[*e*]indole-3-carboxamide, 1-(3,5-difluorophenyl)-3-(4-methoxy-3-(2-(piperidin-1-yl)ethoxy)phenyl)imidazolidin-2-one, *N*-(3-(2-((3-(piperazin-1-yl)pyrazin-2-yl)oxy)ethoxy)benzyl)propan-2-amine		
Drug design technique(s)	**Computational tool(s)**	**References**
Docking into 5-HT_{2C}R model using the X-ray structure of β_2-AR (PDBid 2RH1) as template	FlexX	[137]

Table 2
Ligand-based drug design techniques for the modulation of potential GPCR-derived therapeutic targets of AD

GPCR: Adenosine A_1 receptor (A_1AR)		
Ligands		
N^6-Substituted adenosines, 8-substituted xanthines		
Drug design technique(s)	**Computational tool(s)**	**References**
CoMFA	CHEM-X	[155]
GPCR: Adenosine A_{2A} receptor ($A_{2A}AR$)		
Ligands		
2-(Furan-2-yl)-[1, 2, 4]triazolo[1,5-*f*]pyrimidin-5-amines, 2-(furan-2-yl)-[1, 2, 4]triazolo[1,5-*a*]pyrazin-8-amine, and 2-(furan-2-yl)-[1, 2, 4]triazolo[1,5-*a*][1, 3, 5]triazin-7-amines		
Drug design technique(s)	**Computational tool(s)**	**References**
HQSAR	SYBYL	[154]
Ligands		
Thieno[3,2-*d*]pyrimidine-4-methanones, 4-arylthieno[3,2-*d*]pyrimidines, pyrazolo[3,4-*d*]pyrimidines, pyrrolo[2,3-*d*]pyrimidines, 6-arylpurines, pyrimidine-4-carboxamides, 7-aryltriazolo[4,5-*d*]pyrimidines		
Drug design technique(s)	**Computational tool(s)**	**References**
CoMFA, CoMSIA	SYBYL	[156]
Ligands		
Pyrimidines		
Drug design technique(s)	**Computational tool(s)**	**References**
CoMFA	SYBYL	[157]
Ligands		
2-Substituted adenosines, 2-substituted adenosine-5'uronamides, 2-substituted adenosine-5′*N*-ethyluronamides		
Drug design technique(s)	**Computational tool(s)**	**References**
CoMFA	SYBYL	[158]
Ligands		
Triazolopyrimidines		
Drug design technique(s)	**Computational tool(s)**	**References**
CoMFA	SYBYL	[159]
Ligands		
2-Alkyloxy-, 2-aryloxy-, and 2-aralkyloxy-adenosines		

(continued)

Table 2
(continued)

Drug design technique(s)	**Computational tool(s)**	**References**
CoMFA	CHEM-X	[160]
GPCR: β_2-Adrenergic receptors (β_2-AR)		
Ligands		
Library of 94 β_2-AR agonists and antagonists		
Drug design technique(s)	**Computational tool(s)**	**References**
CoMFA, CoMSIA	SYBYL	[161]
Ligands		
Tryptamines		
Drug design technique(s)	**Computational tool(s)**	**References**
CoMFA	SYBYL	[162]
Ligands		
Fenoterol derivatives		
Drug design technique(s)	**Computational tool(s)**	**References**
CoMFA	SYBYL	[163, 164, 165]
GPCR: CXC motif chemokine receptor 2 ($CXCR_2$)		
Ligands		
N,N′-Diarylsquaramides, *N,N′*-diarylureas, diaminocyclobutenediones		
Drug design technique(s)	**Computational tool(s)**	**References**
CoMFA, CoMSIA	SYBYL	[166]
GPCR: δ-Opioid receptor (DOR)		
Ligands		
SNC80 analogs		
Drug design technique(s)	**Computational tool(s)**	**References**
CoMFA	SYBYL	[167]
GPCR: Histamine H_3 receptor (H_3R)		
Ligands		
Quinolines		
Drug design technique(s)	**Computational tool(s)**	**References**
CoMFA, CoMSIA	SYBYL	[168]
Ligands		

(continued)

Table 2
(continued)

4-(3-(Phenoxy)propyl)-1*H*-imidazoles, 4-aminoquinolines, 3-(1*H*-imidazol-4-yl)propanol derivatives, 1-(4-(phenoxymethyl)benzyl)piperidines		
Drug design technique(s)	**Computational tool(s)**	**References**
CoMFA and CoMSIA combined with the implementation of charged partial surface area and VolSurf descriptors, among others	SYBYL	[169]
Ligands		
Imidazoles, thiazoles		
Drug design technique(s)	**Computational tool(s)**	**References**
CoMFA, CoMSIA	SYBYL	[170]
GPCR: Metabotropic glutamate receptor type 1 ($mGluR_1$)		
Ligands		
Triazafluorenones		
Drug design technique(s)	**Computational tool(s)**	**References**
CoMFA	CERIUS^2	[171]
Ligands		
Quinolines		
Drug design technique(s)	**Computational tool(s)**	**References**
CoMFA	SYBYL	[172]
GPCR: Metabotropic glutamate receptor type 2 ($mGluR_2$)		
Ligands		
Triazolopyridines		
Drug design technique(s)	**Computational tool(s)**	**References**
CoMFA	SYBYL, PIPELINE PILOT	[173]
GPCR: Metabotropic glutamate Receptor type 5 ($mGluR_5$)		
Ligands		
N-(1,3-Diphenyl-1*H*-pyrazol-5-yl)benzamides		
Drug design technique(s)	**Computational tool(s)**	**References**
HQSAR	SYBYL	[174]
Ligands		
Benzodiazepines		
Drug design technique(s)	**Computational tool(s)**	**References**
CoMFA	SYBYL	[175]
Ligands		

(continued)

Table 2
(continued)

Aryl ethers		
Drug design technique(s)	**Computational tool(s)**	**References**
CoMFA	SYBYL	[176]
GPCR: M_2 muscarinic AcetylCholine Receptor (M_2 mAChR)		
Ligands		
Bisquaternary caracurine V derivatives		
Drug design technique(s)	**Computational tool(s)**	**References**
CoMSIA	SYBYL	[177]
Ligands		
Piperidinylpiperidines		
Drug design technique(s)	**Computational tool(s)**	**References**
CoMFA	SYBYL	[178]
GPCR: 5-HydroxyTryptamine 2A Receptor (5-HT_{2A}R)		
Ligands		
Tryptamines		
Drug design technique(s)	**Computational tool(s)**	**References**
HQSAR	SYBYL	[153]
Ligands		
Indoles, methoxybenzenes, quinazolinediones		
Drug design technique(s)	**Computational tool(s)**	**References**
CoMFA, CoMSIA	SYBYL	[179]
Ligands		
1,4-Disubstituted aromatic piperazines		
Drug design technique(s)	**Computational tool(s)**	**References**
CoMFA, CoMSIA	SYBYL	[180]
Ligands		
3-(Aminomethyl)tetralones, ketanserin analogs, 2-aminoethyl benzocyclanones, 2-(2-piperidinoethyl) benzocycloalkanones		
Drug design technique(s)	**Computational tool(s)**	**References**
CoMFA	SYBYL	[181]
Ligands		
Phenylalkylamines		

(continued)

Table 2
(continued)

Drug design technique(s)	**Computational tool(s)**	**References**
CoMFA	SYBYL	[182]
GPCR: 5-HydroxyTryptamine 2C Receptor (5-HT_{2C}R)		
Ligands		
1-(3-Pyridylcarbamoyl)indolines		
Drug design technique(s)	**Computational tool(s)**	**References**
CoMFA	SYBYL	[183]
GPCR: 5-HydroxyTryptamine 4 Receptor (5-HT_4R)		
Ligands		
Benzimidazoles		
Drug design technique(s)	**Computational tool(s)**	**References**
CoMFA	SYBYL	[184, 185]
Ligands		
Indole carbazimidamides, 5-hydroxytryptamine, 4-amino-5-chloro-2-methoxybenzoic acid esters, 4-amino-*N*-[2-(1-aminocycloalkan-1-yl)ethyl]-5-chloro-2-methoxybenzamides, (±)-1-hydroxy-3-aminopyrrolidones, 5-benzyloxytryptamines, 5-methoxytryptamines		
Drug design technique(s)	**Computational tool(s)**	**References**
CoMFA	SYBYL	[186]
Ligands		
Benzamides		
Drug design technique(s)	**Computational tool(s)**	**References**
CoMFA	SYBYL	[187]
GPCR: 5-HydroxyTryptamine 6 Receptor (5-HT_6R)		
Ligands		
Arylsulfonamides		
Drug design technique(s)	**Computational tool(s)**	**References**
HQSAR	HQSAR software	[152]
Ligands		
N_1-Arylsulfonylindoles		
Drug design technique(s)	**Computational tool(s)**	**References**
CoMFA, CoMSIA	SYBYL	[188]

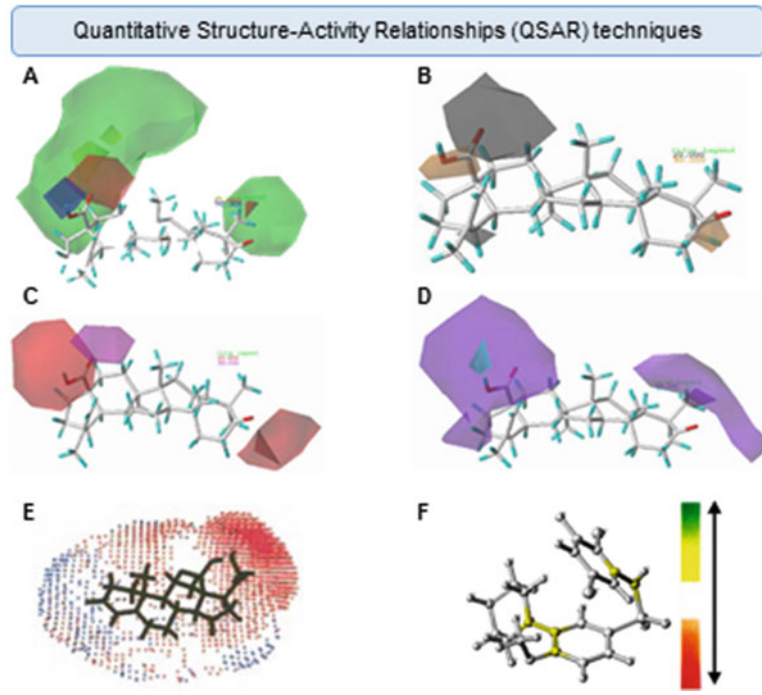

Fig. 3 Representative QSAR-based methodologies for drug design of modulators of potential GPCR-derived therapeutic targets of AD. Color-coded contour maps (**a**) and (**b**) Comparative Molecular Field Analysis (CoMFA) [72], color-coded contour maps (**c**) and (**d**) Comparative Molecular Similarity Index Analysis (CoMSIA) [72], color-coded contour map (**e**) Self-Organizing Molecular Field Analysis (SOMFA) [149], and color-coded contour map (**f**) Hologram Quantitative Structure-Activity Relationship (HQSAR) [152]

compounds with drug-like properties, including Quantitative Structure-Activity Relationship (QSAR) techniques such as Comparative Molecular Field Analysis (CoMFA) (Fig. 3a, b), Comparative Molecular Similarity Index Analysis (CoMSIA) (Fig. 3c, d), Self-Organizing Molecular Field Analysis (SOMFA) (Fig. 3e), and Hologram Quantitative Structure-Activity Relationships (HQSAR) (Fig. 3f).

The investigation of QSARs has been a ligand-based drug design approach of utmost importance for computational chemistry and has opened new perspectives on the drug discovery process. This useful computational methodology searches for mathematical models that explore the contribution of specific functional groups and moieties of the ligands (physicochemical parameters and/or theoretical molecular descriptors) to the experimental determined biological/pharmacological data for congeneric or non-congeneric series of chemical compounds (reviewed in [138, 139, 140]). The development of a robust and trustworthy QSAR model should take into account some considerations, particularly the guarantee that

the chemical structure of all ligands is properly drawn or imported, the reliability of biological/pharmacological activity data, and the use of validated software to calculate the descriptor values. In addition, the biological/pharmacological activity data should possess a normal distribution pattern (reviewed in [138, 139, 140]). The main purposes of QSAR are focused on explaining the subtle differences in biological/pharmacological data, at the molecular level, of a statistical population of drug candidates (training set) through the use of appropriate and relevant molecular descriptors (e.g., topological descriptors, electronic descriptors, geometrical descriptors, constitutional descriptors, etc.) (reviewed in [138, 139, 140]). The construction of mathematical QSAR models usually employs a wide variety of statistical methods for linear modeling, such as multiple (or multivariate) linear regression (MLR) [141], partial least squares (PLS) regression [142], and linear discriminant analysis (LDA) [143], and nonlinear modeling, such as artificial neural networks (ANN) [144] or support vector machines (SVM) [145] to derive a robust mathematical correlation that explains the dependence of particular descriptor variables (independent variables) to the biological/pharmacological activity of a set of ligands (dependent variables). The choice of an appropriate statistical method is crucial especially when a large number of descriptors are calculated in order to neglect the least relevant or redundant descriptors and to select the other ones with the highest mutual intercorrelation with the activity data. The resulting QSAR model is subjected to several validation tests to verify the reliability of the correlation models. After its construction, a QSAR model is usually corroborated by applying multiple strategies of QSAR model validation, in particular the internal validation or cross-validation and the external validation, which provide information about its stability and predictivity (reviewed in [138, 139, 140]). Regarding internal validation or cross-validation, the training set is modified by deleting one (leave-one-out cross-validation, LOO) or more (leave-some-out cross-validation, LSO; leave-many-out cross-validation, LMO) ligands from the set. The QSAR model is reconstructed based on the remaining ligands using the combination of descriptors previously determined, and the biological/pharmacological activity of the eliminated ligand(s) is calculated from the developed QSAR equation. Subsequently, the same procedure is performed until all or a definite portion of the ligands of the training set have been eliminated once and the predictive activity values of the compounds are used for the calculation of several internal validation parameters, in particular the predictive correlation coefficient r^2_{cv} (reviewed in [138, 139, 140]). The external validation consists in the prediction of activity of a group of chemical compounds that are not included in the training set (i.e., test set) and the same parameters are used in the construction of QSAR model. The external predictive ability of the generated QSAR

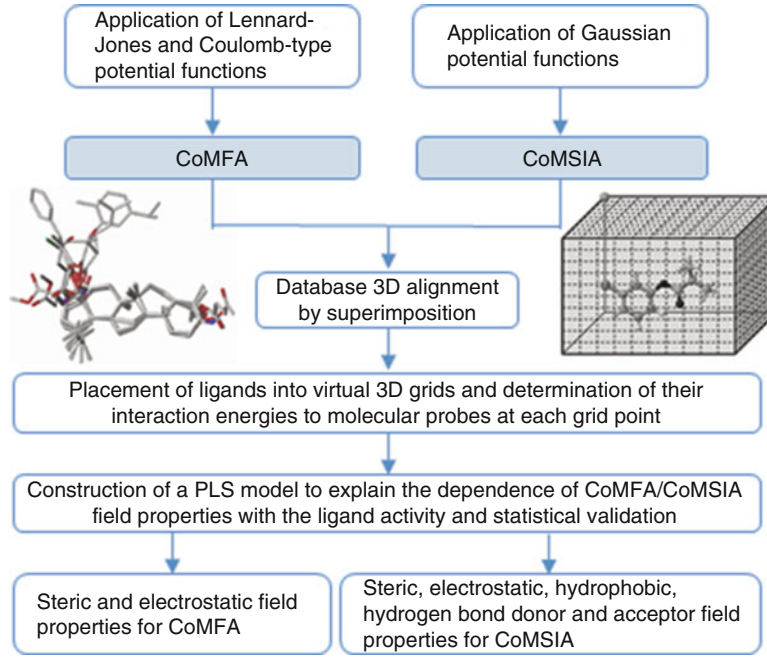

Fig. 4 General procedure for CoMFA and CoMSIA methodologies (Representative images were extracted from [72])

model is determined using the predictive correlation coefficient r^2_{pred} (reviewed in [138, 139, 140]).

The CoMFA and CoMSIA methodologies have been important ligand-based tools for the design and development of more potent drug candidates targeting GPCRs (Fig. 4). The basic concept of CoMFA methodology consists in finding differences in biological/pharmacological activity of a data set of ligands correlated to the differences in their 3D shape and the magnitude of molecular field properties. Particularly, CoMFA is restrained to steric (Lennard-Jones potential functions) and electrostatic components (Coulomb potential functions) for field calculation, and therefore these descriptors only take into account the ability of ligands to establish intermolecular interactions with a putative target protein (enthalpic contributions) [72, 146, 147]. A similar QSAR-based methodology, CoMSIA, was conceived based on arbitrary descriptors, so-called similarity indices. Unlike CoMFA, CoMSIA applies a smoother potential based on Gaussian-type distance-dependent functions, allowing the calculation of various similarity indices, in particular steric, electrostatic, hydrophobic, hydrogen-bond acceptor and donor properties, that were created to cover more broadly than the steric and electrostatic fields calculated by CoMFA, the possible major contributions for the binding free energy of ligands to a putative therapeutic target [148]. The 3D alignment of the chemical structures of ligands is required to

perform both methodologies. An optimal structure alignment of a data set of molecules can be described as the alignment that reaches the maximum superimposition of steric, electrostatic, hydrophobic, hydrogen-bond acceptor and hydrogen-bond donor parameters. In 3D QSAR-based methodologies, the 3D alignment is a crucial step and should reveal the superimposition of molecular conformations that a data set of ligands adopt when interacting with a specific therapeutic target. Each member of the training set is aligned to a template molecule which shares a common molecular substructure, and the members of the aligned training sets are placed inside virtual 3D grid boxes with a default grid spacing in all Cartesian directions [72, 146, 147, 148]. Subsequently, the interaction energies are calculated between the ligands and molecular fragments (molecular probes) at each grid point. Using an appropriate method for regression analysis, usually by PLS, the 3D QSAR model is constructed to describe the variation of biological/pharmacological activity with the variation of CoMFA/CoMSIA interaction fields, and the predictive ability of 3D QSAR model is verified by cross-validation and prediction of activity of test set. The resulting QSAR model is usually interpreted in a graphic form as color-coded contour maps, which exhibit specific volumes of space where the magnitudes of the steric, electrostatic, hydrophobic, hydrogen-bond acceptor and hydrogen-bond donor parameters are positively or negatively correlated with the biological/pharmacological activity [72, 146, 147, 148]. This type of graphical representation can be assumed as a model of the binding site in which a training set of ligands is supposed to interact. While the colored contour maps relative to steric and electrostatic field contributions of CoMFA display the regions of space where the aligned ligands can favorably or unfavorably bind to a putative therapeutic target, the colored contour maps generated by CoMSIA-field contributions highlight the regions of the aligned molecules that can favor the presence of a moiety with a given physicochemical property [148]. From the information provided by these graphical representations of CoMFA/CoMSIA models, the activity of novel synthesized drug candidates can be predicted.

A grid-based 3D QSAR technique known as SOMFA (Fig. 5) was originally developed by *Robinson* et al. to estimate the binding affinity of steroid compounds with corticosteroid-binding globulin [149]. This methodology shares common characteristics with CoMFA, in which a grid-based approach is employed, and with molecular similarity methods, in which the intrinsic molecular properties, such as molecular shape and electrostatic potential, are used to construct SOMFA-based QSAR models [149, 150]. The first step in the SOMFA procedure consists in the determination of mean centered activities for a training set of known ligands. The mean centered activity for each ligand of the training set, which consists in the subtraction of mean activity of the training set from

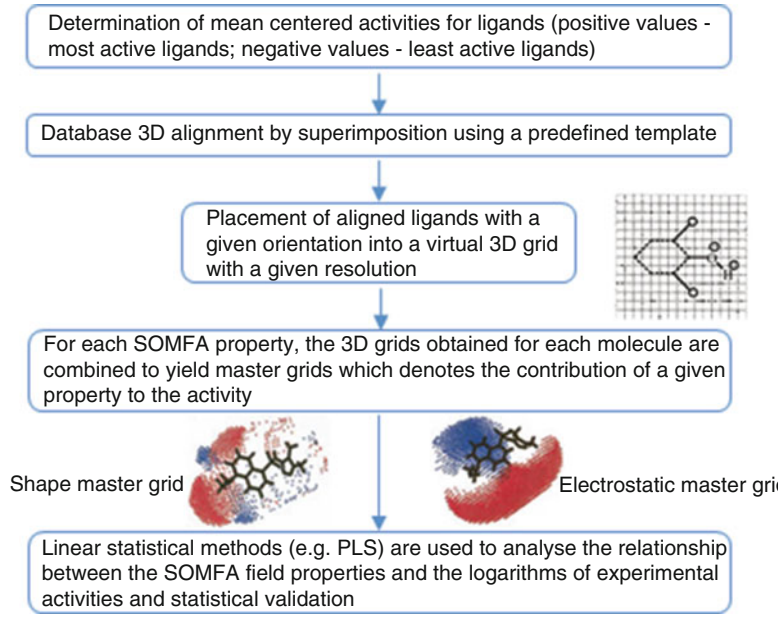

Fig. 5 General procedure for SOMFA methodology (Representative images were extracted from [149])

each ligand's activity, is calculated in order to obtain a scale of activity where the most and the least active ligands present positive and negative values, respectively. In general, the mean centered activity represents a form of descriptor filtering which denotes the structural features that discriminate high-activity from low-activity ligands [149]. Subsequently, the ligands are structurally aligned by superimposition using molecular alignment tools such as principal component analysis (PCA) method and placed on a given orientation into 3D grids with a given resolution, as in other QSAR methodologies, with values at each grid point representing the shape and electrostatic potential. Linear regression models are constructed to describe the dependence of a given SOMFA molecular property with the experimental training set activities represented on logarithmic scale. The calculation of correlation coefficient indicates the potential importance of a given property. The final result is a grid-based map representing each molecular property that can support the molecular design of novel compounds with improved activity (e.g., binding affinity, etc.) [149, 150]. In general, a SOMFA grid can be used to calculate any molecular property. For each molecular property, particularly for molecular shape and electrostatic properties, the grids for each ligand in the training set are combined to yield property master grids that highlight the regions of ligands where steric and electrostatic parameters might be expected to be correlated with the activity (e.g., binding affinity values, etc.) [149]. Highly active

ligands sharing similar structural features superimpose these features at the same point on a master grid. The grid values for highly active ligands strengthen each other, resulting in a final master grid, in which the positive values are associated with common characteristics to these compounds. In a similar way, the least active compounds share common features that lead to a master grid of negative grid values. Since the grid values are assigned based on mean centered activity, moderately active ligands will have small effect on the final grid values. The quality of the model produced in SOMFA increases rapidly with the size of the training set data, and, for that reason, small data sets will not produce the overlapping features for SOMFA, contributing for a lower quality of correlation. The development of SOMFA has been revealed to be advantageous into the search for the best 3D QSAR model due to its speed and simplicity. Additionally, for the construction of a SOMFA model, the structural similarity between the suitably aligned ligands of a training set is not mandatory [149].

HQSAR has emerged as a novel 2D and fragment-based QSAR technique which employs fragment fingerprints as predictive variables of biological/pharmacological activity. The methodology employed in HQSAR procedure (Fig. 6) involves several steps, including the generation of structural fragments for each ligand in the training set and the encoding of these fragments in holograms [151]. Initially, the input molecules are broken into all possible structural fragments of atoms (e.g., linear, branched, cyclic, and

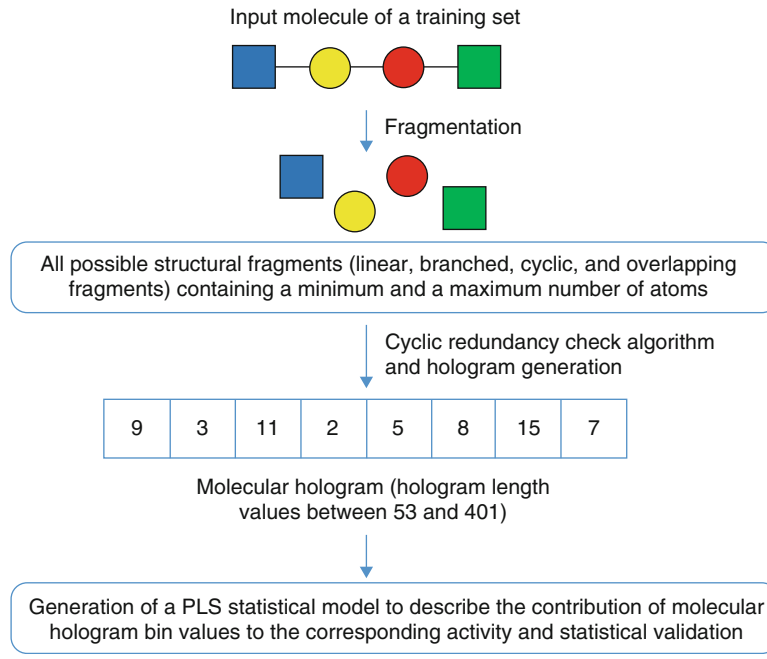

Fig. 6 General procedure for HQSAR methodology

overlapping fragments, etc.) connected in size between a minimum and a maximum number of atoms as defined by hologram length parameters [152, 153, 154]. Afterwards, each unique fragment in the data set is assigned a large positive integer by means of a cyclic redundancy check (CRC) algorithm. Each of these integers corresponds to a square array of integers in a specified hologram length L. The cell values (bin occupancies) are incremented according to the produced fragments. Therefore, all the generated fragments are hashed into boxes (array bins), composing a matrix in the range of 1 to L. The matrix now constitutes a molecular hologram, and the bin occupancies are the descriptor parameters [152, 153, 154]. These descriptors provide some information about chemical and topological features of ligands under study. The use of hashing significantly diminishes the size of the molecular hologram but induces a phenomenon of fragment collision. Upon production of molecular fragments, the identical ones are hashed to the same bin, and the respective bin occupancy is increased. With the objective of avoiding the occurrence of identical or similar fragment collisions between unique molecular fragments, the values of hologram length are often selected to be prime numbers (default hologram length values which are a set of 12 prime numbers ranging from 53 to 401) [152, 153, 154]. The development of HQSAR model is strongly correlated to a number of different parameters concerning hologram generation, in particular the fragment size, the hologram length, and the fragment distinction. Diverse patterns of following fragment distinction parameters, including atom types (A), bond types (B), connectivity (C), hydrogen atoms (H), chirality (Ch), and donors and acceptors (DA), are used for the generation of molecular fragments and for the construction of HQSAR models [152, 153, 154]. Once an optimal model is identified, linear statistical methods such as PLS yield a mathematical equation that explains the dependence of molecular hologram bin values to the corresponding biological/pharmacological activity of each ligand in the training set. The resulting HQSAR models can be graphically displayed as color-coded contribution maps in which the color of each molecular fragment exhibits the contribution (favorable contribution, intermediate contribution, or unfavorable contribution) of an atom or a small number of atoms to the overall activity of ligands under study [152, 153, 154]. As in other QSAR methodologies, the derived HQSAR models are validated, and the biological/pharmacological activities of external test sets are predicted from the generated models. The application of HQSAR as an alternative to the existing QSAR methodologies exhibited a plethora of potential advantages. It avoids the selection and calculation of the physicochemical descriptors by traditional QSAR, and no explicit 3D information for the ligands (e.g., determination of the 3D structure, putative binding conformation, and molecular alignment) is required for the generation of molecular holograms.

Additionally, HQSAR analyses could be easily and rapidly performed for both small and large data sets that are not analyzable by traditional QSAR techniques [152].

3.3 Pharmacophore-Based Drug Design

Pharmacophore modeling has been demonstrated to be a remarkably useful in silico approach for the discovery of potentially bioactive molecules acting on several therapeutic targets [189, 190]. A pharmacophore does not represent a real molecule or an association of functional groups, but it represents an ensemble of steric and electronic determining features that assure an optimal interaction toward a relevant biological/pharmacological target and trigger its biological/pharmacological activity. Therefore, a pharmacophore can be described as the highest common denominator shared by a set of active ligands with similar biological/pharmacological activity and which may interact to the same site of a protein (reviewed in [73]). A pharmacophore model can be developed either in the absence of therapeutic target structure (ligand-based pharmacophore modeling) or based on the 3D structure of a therapeutic target (structure-based pharmacophore modeling) (Fig. 7). The construction of receptor-based pharmacophore models implies the analysis of the pharmacophoric features (hydrogen-bond acceptors and donors, hydrophobic groups, aromatic rings, etc.) in the active site and their spatial relationships which are important for ligand binding (reviewed in [73]). Regarding ligand-based pharmacophore

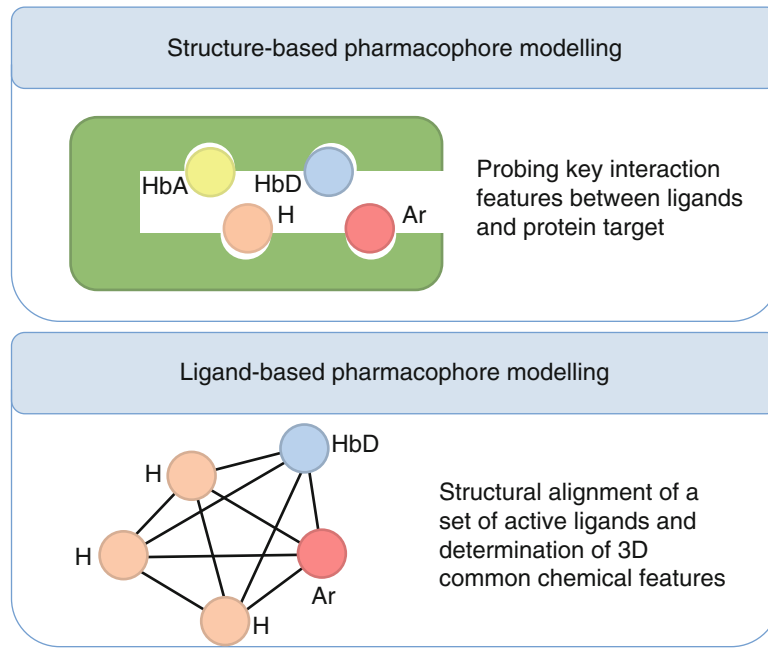

Fig. 7 Representative schemes of structure-based and ligand-based pharmacophore modeling techniques

modeling, the construction of a pharmacophore model involves initially the generation of a conformational space for each ligand of training set to represent their conformational flexibility. The major goal of conformation generation relies on the identification of bioactive conformation(s) of a set of ligands from conformational ensembles in the lowest amount of computational time. Various software tools and algorithms used for conformation generation possess the ability to calculate different conformational geometries containing the bioactive conformation and other similar geometries (reviewed in [73]). A suitable computational tool for conformational search needs to generate all conformational geometries that ligands adopt when they interact with protein targets, to select a short list of low-energy conformational geometries in order to avoid the excess of mass storage capacity and to calculate the conformational geometries in a lower computational time. Subsequently, the multiple ligands belonging to training set are superimposed, and the common 3D structural features crucial for biological/pharmacological activity are determined (reviewed in [73]). Currently, several computational functionalities for generation of pharmacophore models have been developed, including Pharmacophore Alignment and Scoring Engine (PHASE) [191], Activity Prediction Expert System-3D (Apex-3D) [192], MOLMOD [193], System Level Automation Tool for Engineers (SLATE) [194], LigandScout [195], distributed computing (DistComp) [196], SYBYL [197], CATALYST [198], discrete surface charge optimization (DISCO) [198], genetic algorithm for structure and phase production (GASP) [198], and molecular operating environment (MOE) [199], among others. Table 3 reports the most relevant examples of applicability of these software packages for the study of the most critical molecular and electronic features of ligand databases for the modulation of GPCRs with therapeutic potential for AD.

Once a pharmacophore model is created by either ligand-based or structure-based manner, it can be used as a query to perform a virtual screening of 3D chemical databases in the search for new therapeutic strategies for AD based on modulation of GPCRs (reviewed in [73]). In the pharmacophore-based virtual screening procedure, a pharmacophore hypothesis is considered as a template for the identification of hit ligands that present similar chemical features to those of the pharmacophoric template. Apart from the applicability of pharmacophore modeling for virtual screening, de novo drug design approaches have been explored specifically for the design of drug candidates with novel structures which cover the chemical features of a given pharmacophore hypothesis. The software programs of pharmacophore-based de novo drug design usually use as input a set of detached molecular fragments consistent with the pharmacophore hypothesis, and the pharmacophoric fragments are connected by using appropriate linkers (reviewed in [73]).

Table 3
Pharmacophore-based drug design approaches for the modulation of potential GPCR-derived therapeutic targets of AD

GPCR: Adenosine A_{2A} receptor (A_{2A}AR)		
Ligands		
1,2,4-Triazolo[5,1-*i*]purines, 2-*N*-butyl-9-methyl-8-[1–3]triazol-2-yl-9*H*-purin-6-ylamines, pyrazolo[4,3-*e*]-1,2,4-triazolo[1,5-*c*]pyrimidines, 2-amino-6-furan-2-yl-4-substituted nicotinonitriles, 4′-aza-carbocyclic nucleosides, 5,6-dihydro-(9*H*)-pyrazolo[3,4-*c*]-1,2,4-triazolo[4,3-*a*]pyridines, *N*-[6-amino-2-(heteroaryl)pyrimidin-4-yl]acetamides, 4-acetylamino-2-(3,5-dimethylpyrazol-1-yl)-6-pyridylpyrimidines		
Drug design technique(s)	**Computational tool(s)**	**References**
Pharmacophore modeling combined with QSAR	PHASE	[200]
Ligands		
Pyrazolo[4,3-*e*]-1,2,4-triazolo[1,5-*c*]pyrimidines, triazolopyridines, 4-amido-2-aryl-1,2,4-triazolo[4,3-*a*]quinoxalin-1-ones, 2-amino-5-benzoyl-4-(2- furyl)thiazoles, N^2-substituted pyrazolo[3,4-*d*]pyrimidines, 2-(benzimidazol-2-yl)quinoxalines, 5-amino-2-phenyl [1–3]triazolo[1,2-*a*] [1, 2, 4] benzotriazin-1-ones, 1,3-dipropyl-8-(1-heteroarylmethyl-1*H*-pyrazol-4-yl)-xanthines, 9-alkylpurines, pyrido[2,1-*f*]purine-2,4-diones, 1,3-dialkyl-8-*N*-substituted benzyloxycarbonylamino-9-deazaxanthines, 7-aryltriazolo[4,5-*d*]pyrimidines, 7-imino-2-thioxo-3,7-dihydro-2*H*-thiazolo[4,5-*d*] pyrimidines, 2-amino-6-furan-2-yl-4-substituted nicotinonitriles, 2-aminoimidazopyridines, 8-(furan-2-yl)-3-substituted thiazolo[5,4-*e*][1, 2, 4]triazolo-[1,5-*c*]pyrimidine-2(3*H*)-thiones, 2,6-diaryl-4-acylaminopyrimidines, 1,2,4-triazolo[1,5-*c*]pyrimidines, 1,2,4-triazolo[5,1-*i*]purines, *N*-1 monosubstituted 8-(pyrazol-4-yl)xanthenes, 1,3-dialkyl-8-(hetero)aryl-9-OH-9-deazaxanthines, pyrimidine-4-carboxamides, 4-acetylamino-2-(3,5-dimethylpyrazol-1-yl)-6-pyridylpyrimidines		
Drug design technique(s)	**Computational tool(s)**	**References**
Pharmacophore modeling combined with QSAR	PHASE	[201]
Ligands		
7-Substituted 5-amino-2-(2-furyl)pyrazolo[4,3-*e*]-1,2,4-triazolo[1,5-*c*]pyrimidines		
Drug design technique(s)	**Computational tool(s)**	**References**
Pharmacophore modeling	CATALYST	[202]
Ligands		
2,6-Diaryl-4-phenacylaminopyrimidines, 2-amino-*N*-pyrimidin-4-ylacetamides, 2-amino-*N*-pyrimidin-4-yl acetamides, *N*-pyrimidinyl-2-phenoxyacetamides, 4-acetylamino-2-(3,5-dimethylpyrazol-1-yl)-6-pyridylpyrimidines, *N*-[6-amino-2-(heteroaryl)pyrimidin-4-yl]acetamides, pyrazolo[4,3-*e*][1, 2, 4] triazolo[1,5-*c*]pyrimidin-5-amine, pyrazolo[4,3-*e*]-1,2,4-triazolo[1,5-*c*]pyrimidines, 6-(furanyl)-9*H*-purin-2-amines, 2-(2-furanyl)-7-phenyl[1, 2, 4]triazolo[1,5-*c*]pyrimidin-5-amines, 3*H*-[1, 2, 4]-triazolo[5,1-*i*]purin-5-amines, 1,2,4-triazolo[1,5-*c*]pyrimidines, biaryl, heteroaryl, and heterocyclic derivatives of SCH 58261		
Drug design technique(s)	**Computational tool(s)**	**References**
Pharmacophore modeling combined with QSAR based on GFA joined with *k*NN	CATALYST	[203]
GPCR: α_{2A}-Adrenergic receptor (α_{2A}-AR)		

(continued)

Table 3
(continued)

Ligands		
Catecholamines, imidazolines, guanidines, structures possessing distinct scaffolds (rilmenidine, talipexole, xylazyne)		
Drug design technique(s)	**Computational tool(s)**	**References**
Pharmacophore modeling combined with CoMFA	DISCO, SYBYL	[204]
GPCR: CC motif chemokine receptor 2 (CCR_2)		
Ligands		
R-3-amino-pyrrolidines		
Drug design technique(s)	**Computational tool(s)**	**References**
Pharmacophore modeling combined with CoMFA and CoMSIA	SYBYL	[205]
Ligands		
Diaminopropionamide-glycine dipeptides, disubstituted and trisubstituted cyclohexanes		
Drug design technique(s)	**Computational tool(s)**	**References**
Pharmacophore modeling	CATALYST	[206]
GPCR: Corticotropin-releasing factor receptor 1 ($CRFR_1$)		
Ligands		
Arylquinolines, phenylpyrazolo[1,5-*a*]pyrimidines, benzoylpyrimidines, and arylpyrrolopyridines		
Drug design technique(s)	**Computational tool(s)**	**References**
Pharmacophore modeling	CATALYST	[207]
Ligands		
Anilinopyrimidines and triazines		
Drug design technique(s)	**Computational tool(s)**	**References**
Pharmacophore modeling	CATALYST	[208]
Ligands		
N^3-Phenylpyrazinones		
Drug design technique(s)	**Computational tool(s)**	**References**
Pharmacophore modeling	PHASE	[209]
GPCR: δ-Opioid receptor (DOR)		
Ligands		
SB219825, SIOM, (-) TAN-67, BNTX, naltriben, naltrindole, oxymorphindole		
Drug design technique(s)	**Computational tool(s)**	**References**
Pharmacophore modeling	SYBYL	[210]

(continued)

Table 3
(continued)

Ligands		
Non-peptides (xorphanol, naltrindole, BNTX, SIOM, Win44441, lofentanil, carfentanil, SNC80(+8)), cyclic peptides (DPDPE, DPLPE), linear peptides (TIPP, TIP, TI-NH_2)		
Drug design technique(s)	**Computational tool(s)**	**References**
Pharmacophore modeling	DistComp	[196]
Ligands		
(*E*)- and (*Z*)-arylidenenaltrexones		
Drug design technique(s)	**Computational tool(s)**	**References**
Pharmacophore modeling	SYBYL	[211]
Ligands		
DADLE, DPDPE, deltorphins, Leu- and Met-enkephalins, Dmt-Tic, ICI 174,864, TIPP		
Drug design technique(s)	**Computational tool(s)**	**References**
Pharmacophore modeling	SYBYL	[212]
GPCR: Histamine H_3 receptor (H_3R)		
Ligands		
Dibasic biphenyl derivatives, tetrahydroisoquinolines, tetrahydroquinolines, tetrahydroazepines, imidazolidinylidenepropanedinitriles		
Drug design technique(s)	**Computational tool(s)**	**References**
Pharmacophore modeling	CATALYST	[213]
Ligands		
Imidazoles		
Drug design technique(s)	**Computational tool(s)**	**References**
Pharmacophore modeling	SLATE	[214]
Ligands		
1-(4-(3-(Piperidin-1-yl)propoxy)benzyl)piperidine, 1-(4-chlorobenzyl)-1-(5-(pyrrolidin-1-yl)pentyl) guanidine, 3-(2,6-dibromo-4-(2-(dimethylamino)ethyl)phenoxy)-*N*,*N*-dimethylpropan-1-amine		
Drug design technique(s)	**Computational tool(s)**	**References**
Pharmacophore modeling	CATALYST	[215]
GPCR: Metabotropic glutamate receptor type 1 ($mGluR_1$)		
Ligands		
Methylglutamates		
Drug design technique(s)	**Computational tool(s)**	**References**
Pharmacophore modeling	APEX-3D	[216]

(continued)

Table 3
(continued)

Ligands		
α-Substituted cyclobutylglycins, 4-carboxy phenylglycins, (*R*,*S*)-1-aminoindan-2,5-dicarboxylic acid, (±)-α-thioxanthylmethyl-3-carboxycyclobutylglycine		
Drug design technique(s)	**Computational tool(s)**	**References**
Pharmacophore modeling	MOLMOD	[217]
GPCR: Metabotropic glutamate receptor type 2 ($mGluR_2$)		
Ligands		
1,3-Dihydrobenzo[*b*][1, 4]diazepin-2-ones		
Drug design technique(s)	**Computational tool(s)**	**References**
Pharmacophore modeling combined with CoMFA and CoMSIA	DISCO, SYBYL	[218]
Ligands		
Methylglutamates		
Drug design technique(s)	**Computational tool(s)**	**References**
Pharmacophore modeling	APEX-3D	[216]
GPCR: 5-Hydroxytryptamine 2C Receptor ($5\text{-}HT_{2C}R$)		
Ligands		
RS-102221, SB240284, Haloperidol, S20098, 2-alkyl-4-aryl-pyrimidines, bisaryl imidazolidin-2-ones, 2-phenyl-dihydropyrrolones, *N*-substituted-pyridoindolines, *cis*-fused 2-*N*,*N*-dimethylaminomethyl-2,3,3*a*,12*b*-tetrahydrodibenzo[*b*,*f*]furo[2,3-*d*]oxepines, 1*H*-indole-3-carboxylic acid pyridine-3-ylamides, benzazepines		
Drug design technique(s)	**Computational tool(s)**	**References**
Pharmacophore modeling combined with CoMFA	CATALYST, SYBYL	[219]
Ligands		
Library of 16,560 ChemDiv GPCR compounds		
Drug design technique(s)	**Computational tool(s)**	**References**
Pharmacophore modeling	CATALYST	[220]
GPCR: 5-Hydroxytryptamine 4 Receptor ($5\text{-}HT_4R$)		
Ligands		
Indolecarbazimidamide, 3-*N*-isopropylbenzimidazolone amide, 3-*N*-ethylbenzimidazolone amide and benzamide, (*R*)-zacopride, 5-carbamoyltryptamine and metoclopramide		
Drug design technique(s)	**Computational tool(s)**	**References**
Pharmacophore modeling combined with CoMFA	SYBYL	[221]
Ligands		
Indolecarbazimidamides, azabicyclic indole esters, macrocyclic benzamides		
Drug design technique(s)	**Computational tool(s)**	**References**

(continued)

Table 3
(continued)

Pharmacophore modeling	CATALYST	[222]
GPCR: 5-Hydroxytryptamine 6 receptor (5-HT_6R)		
Ligands		
Arylsulfonamides, arylsulfonyl derivatives, *N*-arylsulfonylindoles, 2-substituted tryptamines		
Drug design technique(s)	**Computational tool(s)**	**References**
Pharmacophore modeling	CATALYST	[223]
Ligands		
Indoles; indole-like derivatives; monocyclic, bicyclic, and tricyclic aryl-piperazines; and miscellaneous derivatives		
Drug design technique(s)	**Computational tool(s)**	**References**
Pharmacophore modeling	CATALYST	[224]
Ligands		
2-Methylindoles, 2-phenylindoles		
Drug design technique(s)	**Computational tool(s)**	**References**
Pharmacophore modeling	CATALYST	[225]

GFA genetic function algorithm, *kNN k* nearest neighbor

4 Concluding Remarks

With the progress of the structural biology on elucidation of 3D crystal structures of GPCRs from X-ray crystallography and NMR techniques and of in silico-based drug design tools, a diverse plethora of GPCR modulators have been identified by structure- and ligand-based drug design strategies. Experimentally, the application of structure-based drug design methodologies allows the understanding of ligand-GPCR interactions at a molecular level, which is fundamental for the construction of reliable structure-based pharmacophores and generation of novel drugs. However, future drug candidates acting on GPCRs are likely to rely on ligand-based approaches because of limited structural data information for the majority of GPCRs. The present chapter provided a general overview of the structure- and ligand-based computational methodologies as well as their applicability on various potential GPCR-derived therapeutic targets for AD by small-molecule modulators. In fact, the pharmacological activation/inhibition of all the aforementioned GPCRs on Tables 1, 2, and 3 has provided therapeutic opportunities, and from the analysis of these tables, it has become evident that diverse chemical scaffolds of small molecules have been explored using structure-based, ligand-based, and pharmacophore-

based methodologies in the search for anti-AD alternatives. Collectively, these in silico approaches have revealed to be of utmost importance in early stages of drug discovery, particularly in hit-to-lead optimization of drug candidates, in order to uncover the most favorable molecular modifications for the development of more potent and subtype-selective GPCR modulators targeting AD.

Apart from the extreme relevance of pharmacodynamic (PD) profile of GPCR modulators, pharmacokinetic (PK) properties, including absorption, distribution, metabolism, and excretion (ADME), and toxicology are vital features that should be taken into account in early phases of drug discovery since usually drug candidates with a promising PD profile may be failed at late stages of drug development due to unfavorable PK properties and toxicity. In silico structure- and ligand-based drug design approaches combined with in silico prediction of ADME properties are expected to contribute to the improvement of the computational methodologies used for drug discovery and be fundamental for the development of drugs targeting AD with enhanced PD and PK properties.

Acknowledgments and Funding

This work had the financial support of Fundação para a Ciência e a Tecnologia (FCT/MEC) through national funds and cofinanced by FEDER, under the Partnership Agreement PT2020 (projects UID/QUI/50006/2013 and POCI/01/0145/FEDER/007265). Irina S. Moreira acknowledges support by the FCT – Investigator Programme – IF/00578/2014 (cofinanced by European Social Fund and Programa Operacional Potencial Humano), a Marie Skłodowska-Curie Individual Fellowship MSCA-IF-2015 [MEMBRANEPROT 659826]. This work was also financed by the European Regional Development Fund (ERDF), through the Centro 2020 Regional Operational Programme under project CENTRO-01-0145-FEDER-000008, BrainHealth 2020, and through the COMPETE 2020 – Operational Programme for Competitiveness and Internationalisation and Portuguese national funds via FCT, under project POCI-01-0145-FEDER-007440. Rita Melo acknowledges support from the FCT (SFRH/BPD/97650/2013 and UID/Multi/04349/2013 project). MNDSC further acknowledges FCT for the sabbatical grant SFRH/BSAB/127789/2016.

References

1. Bartus RT (2000) On neurodegenerative diseases, models, and treatment strategies: lessons learned and lessons forgotten a generation following the cholinergic hypothesis. Exp Neurol 163(2):495–529
2. Craig LA, Hong NS, McDonald RJ (2011) Revisiting the cholinergic hypothesis in the development of Alzheimer's disease. Neurosci Biobehav Rev 35(6):1397–1409
3. Hardy J, Selkoe DJ (2002) The amyloid hypothesis of Alzheimer's disease: progress and problems on the road to therapeutics. Science 297(5580):353–356
4. Karran E, Mercken M, Strooper BD (2011) The amyloid cascade hypothesis for Alzheimer's disease: an appraisal for the development of therapeutics. Nat Rev Drug Discov 10(9):698–712
5. Tolnay M, Probst A (1999) Review: *tau* protein pathology in Alzheimer's disease and related disorders. Neuropathol Appl Neurobiol 25(3):171–187
6. Maccioni RB, Farias G, Morales I, Navarrete L (2010) The revitalized *tau* hypothesis on Alzheimer's disease. Arch Med Res 41 (3):226–231
7. Nitsch RM, Deng M, Growdon JH, Wurtman RJ (1996) Serotonin 5-HT_{2A} and 5-HT_{2C} receptors stimulate amyloid precursor protein ectodomain secretion. J Biol Chem 271 (8):4188–4194
8. Price DL, Bonhaus DW, McFarland K (2012) Pimavanserin, a 5-HT_{2A} receptor inverse agonist, reverses psychosis-like behaviors in a rodent model of Alzheimer's disease. Behav Pharmacol 23(4):426–433
9. Arjona AA, Pooler AM, Lee RK, Wurtman RJ (2002) Effect of a 5-HT_{2C} serotonin agonist, dexnorfenfluramine, on amyloid precursor protein metabolism in guinea pigs. Brain Res 951(1):135–140
10. Giannoni P, Gaven F, De Bundel D, Baranger K, Marchetti-Gauthier E, Roman FS, Valjent E, Marin P, Bockaert J, Rivera S (2013) Early administration of RS 67333, a specific 5-HT_4 receptor agonist, prevents amyloidogenesis and behavioral deficits in the 5xFAD mouse model of Alzheimer's disease. Front Aging Neurosci 5:96. doi:10.3389/fnagi.2013.00096. eCollection 2013
11. Pimenova AA, Thathiah A, De Strooper B, Tesseur I (2014) Regulation of amyloid precursor protein processing by serotonin signaling. PLoS One 9(1):e87014. doi:10.1371/journal.pone.0087014
12. Robert SJ, Zugaza JL, Fischmeister R, Gardier AM, Lezoualc'h F (2001) The human serotonin 5-HT_4 receptor regulates secretion of non-amyloidogenic precursor protein. J Biol Chem 276(48):44881–44888
13. Tesseur I, Pimenova AA, Lo AC, Ciesielska M, Lichtenthaler SF, De Maeyer JH, Schuurkes JA, D'Hooge R, De Strooper B (2013) Chronic 5-HT_4 receptor activation decreases Aβ production and deposition in hAPP/PS1 mice. Neurobiol Aging 34 (7):1779–1789
14. Benhamú B, Martín-Fontecha M, Vázquez-Villa H, Pardo L, López-Rodríguez ML (2014) Serotonin 5-HT_6 receptor antagonists for the treatment of cognitive deficiency in Alzheimer's disease. J Med Chem 57 (17):7160–7181
15. Maher-Edwards G, Zvartau-Hind M, Hunter A, Gold M, Hopton G, Jacobs G, Davy M, Williams P (2010) Double-blind, controlled phase II study of a 5-HT_6 receptor antagonist, SB-742457, in Alzheimer's disease. Curr Alzheimer Res 7(5):374–385
16. Rosse G, Schaffhauser H (2010) 5-HT_6 receptor antagonists as potential therapeutics for cognitive impairment. Curr Top Med Chem 10(2):207–221
17. Upton N, Chuang TT, Hunter AJ, Virley DJ (2008) 5-HT_6 receptor antagonists as novel cognitive enhancing agents for Alzheimer's disease. Neurotherapeutics 5(3):458–469
18. Arendash G, Schleif W, Rezai-Zadeh K, Jackson E, Zacharia L, Cracchiolo J, Shippy D, Tan J (2006) Caffeine protects Alzheimer's mice against cognitive impairment and reduces brain β-amyloid production. Neuroscience 142(4):941–952
19. Giunta S, Andriolo V, Castorina A (2014) Dual blockade of the A_1 and A_{2A} adenosine receptor prevents amyloid β toxicity in neuroblastoma cells exposed to aluminum chloride. Int J Biochem Cell Biol 54:122–136
20. Angulo E, Casadó V, Mallol J, Canela EI, Viñals F, Ferrer I, Lluis C, Franco R (2003) A_1 adenosine receptors accumulate in neurodegenerative structures in Alzheimer's disease and mediate both amyloid precursor protein processing and *tau* phosphorylation and translocation. Brain Pathol 13(4):440–451
21. Canas PM, Porciúncula LO, Cunha GM, Silva CG, Machado NJ, Oliveira JM, Oliveira CR, Cunha RA (2009) Adenosine A_{2A} receptor blockade prevents synaptotoxicity and memory dysfunction caused by β-amyloid peptides

via p38 mitogen-activated protein kinase pathway. J Neurosci 29(47):14741–14751

22. Espinosa J, Rocha A, Nunes F, Costa MS, Schein V, Kazlauckas V, Kalinine E, Souza DO, Cunha RA, Porciúncula LO (2013) Caffeine consumption prevents memory impairment, neuronal damage, and adenosine A_{2A} receptors upregulation in the hippocampus of a rat model of sporadic dementia. J Alzheimers Dis 34(2):509–518
23. Nagpure BV, Bian JS (2014) Hydrogen sulfide inhibits A_{2A} adenosine receptor agonist induced β-amyloid production in SH-SY5Y neuroblastoma cells via a cAMP dependent pathway. PLoS One 9(2):e88508. doi:10.1371/journal.pone.0088508. eCollection 2014
24. Orr AG, Hsiao EC, Wang MM, Ho K, Kim DH, Wang X, Guo W, Kang J, Yu GQ, Adame A (2015) Astrocytic adenosine receptor A_{2A} and G_s-coupled signaling regulate memory. Nat Neurosci 18(3):423–434
25. Chen Y, Peng Y, Che P, Gannon M, Liu Y, Li L, Bu G, van Groen T, Jiao K, Wang Q (2014) α_{2A} adrenergic receptor promotes amyloidogenesis through disrupting APP-SorLA interaction. Proc Natl Acad Sci U S A 111 (48):17296–17301
26. Branca C, Wisely EV, Hartman LK, Caccamo A, Oddo S (2014) Administration of a selective β_2 adrenergic receptor antagonist exacerbates neuropathology and cognitive deficits in a mouse model of Alzheimer's disease. Neurobiol Aging 35(12):2726–2735
27. Ni Y, Zhao X, Bao G, Zou L, Teng L, Wang Z, Song M, Xiong J, Bai Y, Pei G (2006) Activation of β_2-adrenergic receptor stimulates γ-secretase activity and accelerates amyloid plaque formation. Nat Med 12 (12):1390–1396
28. Wisely EV, Xiang YK, Oddo S (2014) Genetic suppression of β_2-adrenergic receptors ameliorates *tau* pathology in a mouse model of tauopathies. Hum Mol Genet 23 (15):4024–4034
29. El Khoury J, Toft M, Hickman SE, Means TK, Terada K, Geula C, Luster AD (2007) CCR_2 deficiency impairs microglial accumulation and accelerates progression of Alzheimer-like disease. Nat Med 13(4):432–438
30. Westin K, Buchhave P, Nielsen H, Minthon L, Janciauskiene S, Hansson O (2012) CCL_2 is associated with a faster rate of cognitive decline during early stages of Alzheimer's disease. PLoS One 7(1):e30525. doi:10.1371/journal.pone.0030525
31. Bakshi P, Margenthaler E, Laporte V, Crawford F, Mullan M (2008) Novel role of $CXCR_2$ in regulation of γ-secretase activity. ACS Chem Biol 3(12):777–789
32. Bakshi P, Jin C, Broutin P, Berhane B, Reed J, Mullan M (2009) Structural optimization of a $CXCR_2$-directed antagonist that indirectly inhibits γ-secretase and reduces Aβ. Bioorg Med Chem 17(23):8102–8112
33. Bakshi P, Margenthaler E, Reed J, Crawford F, Mullan M (2011) Depletion of $CXCR_2$ inhibits γ-secretase activity and amyloid-β production in a murine model of Alzheimer's disease. Cytokine 53(2):163–169
34. Carroll JC, Iba M, Bangasser DA, Valentino RJ, James MJ, Brunden KR, Lee VMY, Trojanowski JQ (2011) Chronic stress exacerbates *tau* pathology, neurodegeneration, and cognitive performance through a corticotropin-releasing factor receptor-dependent mechanism in a transgenic mouse model of tauopathy. J Neurosci 31 (40):14436–14449
35. Justice NJ, Huang L, Tian JB, Cole A, Pruski M, Hunt AJ, Flores R, Zhu MX, Arenkiel BR, Zheng H (2015) Posttraumatic stress disorder-like induction elevates β-amyloid levels, which directly activates corticotropin-releasing factor neurons to exacerbate stress responses. J Neurosci 35(6):2612–2623
36. Rissman RA, Staup MA, Lee AR, Justice NJ, Rice KC, Vale W, Sawchenko PE (2012) Corticotropin-releasing factor receptor-dependent effects of repeated stress on *tau* phosphorylation, solubility, and aggregation. Proc Natl Acad Sci U S A 109 (16):6277–6282
37. Scullion GA, Hewitt KN, Pardon MC (2013) Corticotropin-releasing factor receptor 1 activation during exposure to novelty stress protects against Alzheimer's disease-like cognitive decline in AβPP/PS1 mice. J Alzheimers Dis 34(3):781–793
38. Cai Z, Ratka A (2012) Opioid system and Alzheimer's disease. NeuroMolecular Med 14(2):91–111
39. Medhurst AD, Atkins AR, Beresford IJ, Brackenborough K, Briggs MA, Calver AR, Cilia J, Cluderay JE, Crook B, Davis JB, Davis RK, Davis RP, Dawson LA, Foley AG, Gartlon J, Gonzalez MI, Heslop T, Hirst WD, Jennings C, Jones DNC, Lacroix LP, Martyn A, Ociepka S, Ray A, Regan CM, Roberts JC, Schogger J, Southam E, Stean TO, Trail BK, Upton N, Wadsworth G, Wald JA, White T, Witherington J, Woolley ML, Worby A,

Wilson DM (2007) GSK189254, a novel H_3 receptor antagonist that binds to histamine H_3 receptors in Alzheimer's disease brain and improves cognitive performance in preclinical models. J Pharm Exp Ther 321 (3):1032–1045

40. Nathan PJ, Boardley R, Scott N, Berges A, Maruff P, Sivananthan T, Upton N, Lowy MT, Nestor PJ, Lai R (2013) The safety, tolerability, pharmacokinetics and cognitive effects of GSK239512, a selective histamine H_3 receptor antagonist in patients with mild to moderate Alzheimer's disease: a preliminary investigation. Curr Alzheimer Res 10 (3):240–251
41. Haig GM, Pritchett Y, Meier A, Othman AA, Hall C, Gault LM, Lenz RA (2014) A randomized study of H_3 antagonist ABT-288 in mild-to-moderate Alzheimer's dementia. J Alzheimer Dis 42(3):959–971
42. Kim SH, Fraser PE, Westaway D, George-Hyslop PHS, Ehrlich ME, Gandy S (2010) Group II metabotropic glutamate receptor stimulation triggers production and release of Alzheimer's amyloid β42 from isolated intact nerve terminals. J Neurosci 30 (11):3870–3875
43. Kirazov L, Löffler T, Schliebs R, Bigl V (1997) Glutamate-stimulated secretion of amyloid precursor protein from cortical rat brain slices. Neurochem Int 30(6):557–563
44. Lee R, Wurtman RJ, Cox AJ, Nitsch RM (1995) Amyloid precursor protein processing is stimulated by metabotropic glutamate receptors. Proc Natl Acad Sci U S A 92 (17):8083–8087
45. Nitsch RM, Deng A, Wurtman RJ, Growdon JH (1997) Metabotropic glutamate receptor subtype $mGluR_{1\alpha}$ stimulates the secretion of the amyloid β-protein precursor ectodomain. J Neurochem 69(2):704–712
46. Lee HG, Zhu X, Casadesus G, Pallàs M, Camins A, O'Neill MJ, Nakanishi S, Perry G, Smith MA (2009) The effect of $mGluR_2$ activation on signal transduction pathways and neuronal cell survival. Brain Res 1249:244–250
47. Spinelli S, Ballard T, Gatti-McArthur S, Richards GJ, Kapps M, Woltering T, Wichmann J, Stadler H, Feldon J, Pryce CR (2005) Effects of the $mGluR_{2/3}$ agonist LY354740 on computerized tasks of attention and working memory in marmoset monkeys. Psychopharmacol 179(1):292–302
48. Um JW, Kaufman AC, Kostylev M, Heiss JK, Stagi M, Takahashi H, Kerrisk ME, Vortmeyer A, Wisniewski T, Koleske AJ, Gunther EC, Nygaard HB, Strittmatter SM (2013) Metabotropic glutamate receptor 5 is a coreceptor for Alzheimer Aβ oligomer bound to cellular prion protein. Neuron 79 (5):887–902
49. Kumar A, Dhull DK, Mishra PS (2015) Therapeutic potential of $mGluR_5$ targeting in Alzheimer's disease. Front Neurosci 9:215. doi:10.3389/fnins.2015.00215
50. Caccamo A, Oddo S, Billings LM, Green KN, Martinez-Coria H, Fisher A, LaFerla FM (2006) M_1 receptors play a central role in modulating AD-like pathology in transgenic mice. Neuron 49(5):671–682
51. Davis AA, Fritz JJ, Wess J, Lah JJ, Levey AI (2010) Deletion of M_1 muscarinic acetylcholine receptors increases amyloid pathology *in vitro* and *in vivo*. J Neurosci 30 (12):4190–4196
52. Jiang S, Wang Y, Ma Q, Zhou A, Zhang X, Zhang YW (2012) M_1 muscarinic acetylcholine receptor interacts with BACE1 and regulates its proteosomal degradation. Neurosci Lett 515(2):125–130
53. Nitsch RM, Slack BE, Wurtman RJ, Growdon JH (1992) Release of Alzheimer amyloid precursor derivatives stimulated by activation of muscarinic acetylcholine receptors. Science 258(5080):304–307
54. Züchner T, Perez-Polo JR, Schliebs R (2004) β-secretase BACE1 is differentially controlled through muscarinic acetylcholine receptor signaling. J Neurosci Res 77(2):250–257
55. Packard MG, Regenold W, Quirion R, White NM (1990) Post-training injection of the acetylcholine M_2 receptor antagonist AF-DX 116 improves memory. Brain Res 524(1):72–76
56. Han Y, Moreira IS, Urizar E, Weinstein H, Javitch JA (2009) Allosteric communication between protomers of dopamine class a GPCR dimers modulates activation. Nat Chem Biol 5(9):688–695
57. Moreira IS (2014) Structural features of the G-protein/GPCR interactions. Biochim Biophys Acta, Gen Subj 1840(1):16–33
58. Schioth HB, Fredriksson R (2005) The GRAFS classification system of G-protein coupled receptors in comparative perspective. Gen Comp Endocrinol 142(1–2):94–101
59. Ji TH, Grossmann M, Ji I (1998) G protein-coupled receptors. I. Diversity of receptor-ligand interactions. J Biol Chem 273 (28):17299–17302
60. Rosenbaum DM, Rasmussen SG, Kobilka BK (2009) The structure and function of G-protein-coupled receptors. Nature 459 (7245):356–363

61. Lang M, Beck-Sickinger AG (2006) Structure-activity relationship studies: methods and ligand design for G-protein coupled peptide receptors. Curr Protein Pept Sci 7 (4):335–353
62. Marinissen MJ, Gutkind JS (2001) G-protein-coupled receptors and signaling networks: emerging paradigms. Trends Pharmacol Sci 22(7):368–376
63. Birnbaumer L (2007) The discovery of signal transduction by G proteins. A personal account and an overview of the initial findings and contributions that led to our present understanding. Biochim Biophys Acta Biomembr 1768(4):756–771
64. Kontoyianni M, Liu Z (2012) Structure-based design in the GPCR target space. Curr Med Chem 19(4):544–556
65. Shukla AK, Xiao K, Lefkowitz RJ (2011) Emerging paradigms of β-arrestin-dependent seven transmembrane receptor signaling. Trends Biochem Sci 36(9):457–469
66. Lefkowitz RJ (1998) G protein-coupled receptors. III New roles for receptor kinases and β-arrestins in receptor signaling and desensitization. J Biol Chem 273 (30):18677–18680
67. Wolfe BL, Trejo J (2007) Clathrin-dependent mechanisms of G protein-coupled receptor endocytosis. Traffic 8(5):462–470
68. Tsao P, von Zastrow M (2000) Downregulation of G protein-coupled receptors. Curr Opin Neurobiol 10(3):365–369
69. Collins S, Caron MG, Lefkowitz RJ (1991) Regulation of adrenergic receptor responsiveness through modulation of receptor gene expression. Annu Rev Physiol 53:497–508
70. De Vries L, Zheng B, Fischer T, Elenko E, Farquhar MG (2000) The regulator of G protein signaling family. Annu Rev Pharmacol Toxicol 40:235–271
71. Ross EM, Wilkie TM (2000) GTPase-activating proteins for heterotrimeric G proteins: regulators of G protein signaling (RGS) and RGS-like proteins. Annu Rev Biochem 69:795–827
72. Ghemtio L, Zhang Y, Xhaard H (2012) CoMFA/CoMSIA and pharmacophore modelling as a powerful tools for efficient virtual screening: application to anti-leishmanial betulin derivatives. In: Taha MO (ed) Virtual screening. In Tech, Croatia, pp 55–82. doi:10.5772/36690
73. Yang SY (2010) Pharmacophore modeling and applications in drug discovery: challenges and recent advances. Drug Discov Today 15 (11–12):444–450
74. Ghosh E, Kumari P, Jaiman D, Shukla AK (2015) Methodological advances: the unsung heroes of the GPCR structural revolution. Nat Rev Mol Cell Biol 16(2):69–81
75. Palczewski K, Kumasaka T, Hori T, Behnke CA, Motoshima H, Fox BA, Le Trong I, Teller DC, Okada T, Stenkamp RE, Yamamoto M, Miyano M (2000) Crystal structure of rhodopsin: a G protein-coupled receptor. Science 289(5480):739–745
76. Costanzi S, Siegel J, Tikhonova IG, Jacobson KA (2009) Rhodopsin and the others: a historical perspective on structural studies of G protein-coupled receptors. Curr Pharm Des 15(35):3994–4002
77. Patny A, Desai PV, Avery MA (2006) Homology modeling of G-protein-coupled receptors and implications in drug design. Curr Med Chem 13(14):1667–1691
78. Cherezov V, Rosenbaum DM, Hanson MA, Rasmussen SG, Thian FS, Kobilka TS, Choi HJ, Kuhn P, Weis WI, Kobilka BK, Stevens RC (2007) High-resolution crystal structure of an engineered human β_2-adrenergic G protein-coupled receptor. Science 318 (5854):1258–1265
79. Rasmussen SG, Choi HJ, Rosenbaum DM, Kobilka TS, Thian FS, Edwards PC, Burghammer M, Ratnala VR, Sanishvili R, Fischetti RF, Schertler GF, Weis WI, Kobilka BK (2007) Crystal structure of the human β_2 adrenergic G-protein-coupled receptor. Nature 450(7168):383–387
80. Warne T, Serrano-Vega MJ, Baker JG, Moukhametzianov R, Edwards PC, Henderson R, Leslie AG, Tate CG, Schertler GF (2008) Structure of a β_1-adrenergic G-protein-coupled receptor. Nature 454(7203):486–491
81. Christopoulos A (2002) Allosteric binding sites on cell-surface receptors: novel targets for drug discovery. Nat Rev Drug Discov 1 (3):198–210
82. Conn PJ, Christopoulos A, Lindsley CW (2009) Allosteric modulators of GPCRs: a novel approach for the treatment of CNS disorders. Nat Rev Drug Discov 8(1):41–54
83. Chang SD, Bruchas MR (2014) Functional selectivity at GPCRs: new opportunities in psychiatric drug discovery. Neuropsychopharmacol 39(1):248–249
84. Schrage R, Kostenis E (2017) Functional selectivity and dualsteric/bitopic GPCR targeting. Curr Opin Pharmacol 32:85–90
85. Vishnivetskiy SA, Gimenez LE, Francis DJ, Hanson SM, Hubbeil WL, Klug CS, Gurevich VV (2011) Few residues within an extensive binding interface drive receptor interaction

and determine the specificity of arrestin proteins. J Biol Chem 286(27):24288–24299

86. Rasmussen SG, DeVree BT, Zou Y, Kruse AC, Chung KY, Kobilka TS, Thian FS, Chae PS, Pardon E, Calinski D, Mathiesen JM, Shah ST, Lyons JA, Caffrey M, Gellman SH, Steyaert J, Skiniotis G, Weis WI, Sunahara RK, Kobilka BK (2011) Crystal structure of the β_2 adrenergic receptor-G_s protein complex. Nature 477(7366):549–555
87. Dror RO, Arlow DH, Maragakis P, Mildorf TJ, Pan AC, Xu H, Borhani DW, Shaw DE (2011) Activation mechanism of the β_2-adrenergic receptor. Proc Natl Acad Sci U S A 108(46):18684–18689
88. Kohlhoff KJ, Shukla D, Lawrenz M, Bowman GR, Konerding DE, Belov D, Altman RB, Pande VS (2014) Cloud-based simulations on Google Exacycle reveal ligand modulation of GPCR activation pathways. Nat Chem 6 (1):15–21
89. Bruno A, Costantino G (2012) Molecular dynamics simulations of G protein-coupled receptors. Mol Inform 31(3–4):222–230
90. Cozzini P, Kellogg GE, Spyrakis F, Abraham DJ, Costantino G, Emerson A, Fanelli F, Gohlke H, Kuhn LA, Morris GM, Orozco M, Pertinhez TA, Rizzi M, Sotriffer CA (2008) Target flexibility: an emerging consideration in drug discovery and design. J Med Chem 51(20):6237–6255
91. Feixas F, Lindert S, Sinko W, McCammon JA (2014) Exploring the role of receptor flexibility in structure-based drug discovery. Biophys Chem 186:31–45
92. Jo S, Lim JB, Klauda JB, Im W (2009) CHARMM-GUI membrane builder for mixed bilayers and its application to yeast membranes. Biophys J 97(1):50–58
93. Wu EL, Cheng X, Jo S, Rui H, Song KC, Dávila-Contreras EM, Qi Y, Lee J, Monje-Galvan V, Venable RM, Klauda JB, Im W (2014) CHARMM-GUI *Membrane Builder* toward realistic biological membrane simulations. J Comput Chem 35(27):1997–2004
94. Ribeiro JV, Bernardi RC, Rudack T, Stone JE, Phillips JC, Freddolino PL, Schulten K (2016) QwikMD - integrative molecular dynamics toolkit for novices and experts. Sci Rep 6:26536. doi:10.1038/srep26536
95. Doerr S, Harvey MJ, Noé F, De Fabritiis G (2016) HTMD: high-throughput molecular dynamics for molecular discovery. J Chem Theory Comput 12(4):1845–1852
96. Guo W, Shi L, Filizola M, Weinstein H, Javitch JA (2005) Crosstalk in G protein-coupled receptors: changes at the transmembrane homodimer interface determine activation. Proc Natl Acad Sci U S A 102(48):17495–17500
97. Kitchen DB, Decornez H, Furr JR, Bajorath J (2004) Docking and scoring in virtual screening for drug discovery: methods and applications. Nat Rev Drug Discov 3(11):935–949
98. Morris GM, Huey R, Olson AJ (2008) Using AutoDock for ligand-receptor docking. Curr Protoc Bioinformatics 24:8.14:8.14.1–8.14.40. doi:10.1002/0471250953.bi0814s24
99. Trott O, Olson AJ (2010) AutoDock Vina: improving the speed and accuracy of docking with a new scoring function, efficient optimization, and multithreading. J Comput Chem 31(2):455–461
100. Wu G, Robertson DH, Brooks CL 3rd, Vieth M (2003) Detailed analysis of grid-based molecular docking: a case study of CDOCKER-A CHARMm-based MD docking algorithm. J Comput Chem 24 (13):1549–1562
101. Rarey M, Kramer B, Lengauer T, Klebe G (1996) A fast flexible docking method using an incremental construction algorithm. J Mol Biol 261(3):470–489
102. Verdonk ML, Cole JC, Hartshorn MJ, Murray CW, Taylor RD (2003) Improved protein-ligand docking using GOLD. Proteins 52 (4):609–623
103. Repasky MP, Shelley M, Friesner RA (2007) Flexible ligand docking with GLIDE. Curr Protoc Bioinformatics 18:8.12:8.12.1–8.12.36. doi:10.1002/0471250953.bi0812s18
104. Neves MA, Totrov M, Abagyan R (2012) Docking and scoring with ICM: the benchmarking results and strategies for improvement. J Comput Aided Mol Des 26 (6):675–686
105. Marcou G, Rognan D (2007) Optimizing fragment and scaffold docking by use of molecular interaction fingerprints. J Chem Inf Model 47(1):195–207
106. Kalid O, Toledo Warshaviak D, Shechter S, Sherman W, Shacham S (2012) Consensus induced fit docking (cIFD): methodology, validation, and application to the discovery of novel CRM1 inhibitors. J Comput Aided Mol Des 26(11):1217–1228
107. Rao SN, Head MS, Kulkarni A, LaLonde JM (2007) Validation studies of the site-directed docking program LibDock. J Chem Inf Model 47(6):2159–2171
108. Bai Q, Shao Y, Pan D, Zhang Y, Liu H, Yao X (2014) Search for β_2 adrenergic receptor

ligands by virtual screening via grid computing and investigation of binding modes by docking and molecular dynamics simulations. PLoS One 9(9):e107837. doi:10.1371/journal.pone.0107837. eCollection 2014

109. Korb O, Stutzle T, Exner TE (2009) Empirical scoring functions for advanced protein-ligand docking with PLANTS. J Chem Inf Model 49(1):84–96
110. Gutiérrez-de-Terán H, Centeno NB, Pastor M, Sanz F (2004) Novel approaches for modeling of the A_1 adenosine receptor and its agonist binding site. Proteins: Struct Funct Bioinf 54(4):705–715
111. Kolb P, Phan K, Gao ZG, Marko AC, Sali A, Jacobson KA (2012) Limits of ligand selectivity from docking to models: in Silico screening for A_1 adenosine receptor antagonists. PLoS One 7(11):e49910. doi:10.1371/journal.pone.0049910
112. Ke YR, Jin HW, Liu ZM, Zhang LR (2010) Homology modeling and structure validation of the adenosine A_1 receptor. Acta Phys - Chim Sin 26(10):2833–2839
113. Langmead CJ, Andrews SP, Congreve M, Errey JC, Hurrell E, Marshall FH, Mason JS, Richardson CM, Robertson N, Zhukov A, Weir M (2012) Identification of novel adenosine A_{2A} receptor antagonists by virtual screening. J Med Chem 55(5):1904–1909
114. Katritch V, Jaakola VP, Lane J, Lin J, Ijzerman AP, Yeager M, Kufareva I, Stevens RC, Abagyan R (2010) Structure-based discovery of novel chemotypes for adenosine A_{2A} receptor antagonists. J Med Chem 53(4):1799–1809
115. Ivanov AA, Barak D, Jacobson KA (2009) Evaluation of homology modeling of G-protein-coupled receptors in light of the A_{2A} adenosine receptor crystallographic structure. J Med Chem 52(10):3284–3292
116. Rodríguez D, Gao ZG, Moss SM, Jacobson KA, Carlsson J (2015) Molecular docking screening using agonist-bound GPCR structures: probing the A_{2A} adenosine receptor. J Chem Inf Model 55(3):550–563
117. Carlsson J, Yoo L, Gao ZG, Irwin JJ, Shoichet BK, Jacobson KA (2010) Structure-based discovery of A_{2A} adenosine receptor ligands. J Med Chem 53(9):3748–3755
118. Ostopovici-Halip L, Curpăn R, Mracec M, Bologa CG (2011) Structural determinants of the α_2 adrenoceptor subtype selectivity. J Mol Graph Model 29(8):1030–1038
119. Jayaraman A, Jamil K, Kakarala KK (2013) Homology modelling and docking studies of human α_2-adrenergic receptor subtypes. J Comput Sci Syst Biol 6:136–149
120. Kooistra AJ, Vischer HF, McNaught-Flores D, Leurs R, de Esch IJP, de Graaf C (2016) Function-specific virtual screening for GPCR ligands using a combined scoring method. Sci Rep 6:28288. doi:10.1038/srep28288
121. Kolb P, Rosenbaum DM, Irwin JJ, Fung JJ, Kobilka BK, Shoichet BK (2009) Structure-based discovery of β_2-adrenergic receptor ligands. Proc Natl Acad Sci U S A 106 (16):6843–6848
122. Kothandan G, Gadhe CG, Cho SJ (2012) Structural insights from binding poses of CCR_2 and CCR_5 with clinically important antagonists: a combined in silico study. PLoS One 7(3):e32864. doi:10.1371/journal.pone.0032864
123. Singh R, Sobhia ME (2013) Structure prediction and molecular dynamics simulations of a G-protein coupled receptor: human CCR_2 receptor. J Biomol Struct Dyn 31 (7):694–715
124. Di Fabio R, Arban R, Bernasconi G, Braggio S, Blaney FE, Capelli AM, Castiglioni E, Donati D, Fazzolari E, Ratti E, Feriani A, Contini S, Gentile G, Ghirlanda D, Sabbatini FM, Andreotti D, Spada S, Marchioro C, Worby A, St-Denis Y (2008) Dihydropyrrole [2,3-*d*]pyridine derivatives as novel corticotropin-releasing factor-1 antagonists: mapping of the receptor binding pocket by in silico docking studies. J Med Chem 51 (22):7273–7286
125. Micovic V, Ivanovic MD, Dosen-Micovic L (2009) Docking studies suggest ligand-specific δ-opioid receptor conformations. J Mol Model 15(3):267–280
126. Bautista DL, Asher W, Carpenter L (2005) Development of the human μ-, κ-, and δ-opioid receptors and docking with morphine. J Ky Acad Sci 66(2):107–117
127. Sirci F, Istyastono EP, Vischer HF, Kooistra AJ, Nijmeijer S, Kuijer M, Wijtmans M, Mannhold R, Leurs R, de Esch IJP, de Graaf C (2012) Virtual fragment screening: discovery of histamine H_3 receptor ligands using ligand-based and protein-based molecular fingerprints. J Chem Inf Model 52 (12):3308–3324
128. Schlegel B, Laggner C, Meier R, Langer T, Schnell D, Seifert R, Stark H, Höltje HD, Sippl W (2007) Generation of a homology model of the human histamine H_3 receptor for ligand docking and pharmacophore-based screening. J Comput Aided Mol Des 21 (8):437–453
129. Levoin N, Calmels T, Poupardin-Olivier O, Labeeuw O, Danvy D, Robert P, Berrebi-Bertrand I, Ganellin CR, Schunack W, Stark

H, Capet M (2008) Refined docking as a valuable tool for lead optimization: application to histamine H_3 receptor antagonists. Arch Pharm (Weinheim) 341(10):610–623

130. Costantino G, Pellicciari R (1996) Homology modeling of metabotropic glutamate receptors. (mGluRs) structural motifs affecting binding modes and pharmacological profile of $mGluR_1$ agonists and competitive antagonists. J Med Chem 39(20):3998–4006
131. Chin SP, Buckle MJ, Chalmers DK, Yuriev E, Doughty SW (2014) Toward activated homology models of the human M_1 muscarinic acetylcholine receptor. J Mol Graph Model 49:91–98
132. Swaminathan M, Chee CF, Chin SP, Buckle MJ, Rahman NA, Doughty SW, Chung LY (2014) Flavonoids with M_1 muscarinic acetylcholine receptor binding activity. Molecules 19(7):8933–8948
133. Kruse AC, Weiss DR, Rossi M, Hu J, Hu K, Eitel K, Gmeiner P, Wess J, Kobilka BK, Shoichet BK (2013) Muscarinic receptors as model targets and antitargets for structure-based ligand discovery. Mol Pharmacol 84 (4):528–540
134. Gandhimathi A, Sowdhamini R (2016) Molecular modelling of human 5-hydroxytryptamine receptor ($5\text{-}HT_{2A}$) and virtual screening studies towards the identification of agonist and antagonist molecules. J Biomol Struct Dyn 34(5):952–970
135. Kanagarajadurai K, Malini M, Bhattacharya A, Panicker MM, Sowdhamini R (2009) Molecular modeling and docking studies of human 5-hydroxytryptamine 2A ($5\text{-}HT_{2A}$) receptor for the identification of hotspots for ligand binding. Mol BioSyst 5(12):1877–1888
136. Brea J, Rodrigo J, Carrieri A, Sanz F, Cadavid MI, Enguix MJ, Villazón M, Mengod G, Caro Y, Masaguer CF, Raviña E, Centeno NB, Carotti A, Loza MI (2002) New serotonin $5\text{-}HT_{2A}$, $5\text{-}HT_{2B}$, and $5\text{-}HT_{2C}$ receptor antagonists: synthesis, pharmacology, 3D-QSAR, and molecular modeling of (aminoalkyl)benzo and heterocycloalkanones. J Med Chem 45(1):54–71
137. Ahmed A, Nagarajan S, Doddareddy MR, Cho YS, Pae AN (2011) Binding mode prediction of 5-hydroxytryptamine 2C receptor ligands by homology modeling and molecular docking analysis. Bull Kor Chem Soc 32 (6):2008–2014
138. Perkins R, Fang H, Tong W, Welsh WJ (2003) Quantitative structure-activity relationship methods: perspectives on drug discovery and toxicology. Environ Toxicol Chem 22(8):1666–1679
139. Dudek AZ, Arodz T, Galvez J (2006) Computational methods in developing quantitative structure-activity relationships (QSAR): a review. Comb Chem High Throughput Screen 9(3):213–228
140. Roy K, Kar S, Das RN (2015) Statistical methods in QSAR/QSPR. In: A primer on QSAR/QSPR modeling. SpringerBriefs in Molecular Science, Cham, pp 37–59
141. Alexopoulos EC (2010) Introduction to multivariate regression analysis. Hippokratia 14 (1):23–28
142. Abdi H (2003) Partial least square regression (PLS regression). In: Lewis-Beck M et al (eds) Encyclopedia of social sciences research methods. Sage, Thousand Oaks, pp 792–795
143. Speck-Planche A, Kleandrova VV, Luan F, Cordeiro MN (2013) Multi-target inhibitors for proteins associated with Alzheimer: in silico discovery using fragment-based descriptors. Curr Alzheimer Res 10(2):117–124
144. Speck-Planche A, Kleandrova VV (2012) QSAR and molecular docking techniques for the discovery of potent monoamine oxidase B inhibitors: computer-aided generation of new rasagiline bioisosteres. Curr Top Med Chem 12(16):1734–1747
145. Chapelle O, Vapnik V, Bousquet O, Mukherjee S (2002) Choosing multiple parameters for support vector machines. Mach Learn 46 (1):131–159
146. Cramer RD, Patterson DE, Bunce JD (1988) Comparative molecular field analysis (CoMFA). 1. Effect of shape on binding of steroids to carrier proteins. J Am Chem Soc 110(18):5959–5967
147. Kubinyi H (2008) Comparative molecular field analysis (CoMFA). In: Gasteiger J (ed) Handbook of Chemoinformatics: from data to knowledge in 4 volumes. Wiley-VCH Verlag GmbH, Weinheim, pp 1555–1574. doi:10.1002/9783527618279.ch44d
148. Klebe G, Abraham U, Mietzner T (1994) Molecular similarity indices in a comparative analysis (CoMSIA) of drug molecules to correlate and predict their biological activity. J Med Chem 37(24):4130–4146
149. Robinson DD, Winn PJ, Lyne PD, Richards WG (1999) Self-organizing molecular field analysis: a tool for structure-activity studies. J Med Chem 42(4):573–583
150. Li M, Du L, Wu B, Xia L (2003) Self-organizing molecular field analysis on α_{1A}-adrenoreceptor dihydropyridine antagonists. Bioorg Med Chem 11(18):3945–3951
151. Moda TL, Montanari CA, Andricopulo AD (2007) Hologram QSAR model for the

prediction of human oral bioavailability. Bioorg Med Chem 15:7738–7745

152. Doddareddy MR, Lee YJ, Cho YS, Choi KI, KohHY PAN (2004) Hologram quantitative structure activity relationship studies on 5-HT_6 antagonists. Bioorg Med Chem 12 (14):3815–3824
153. Palangsuntikul R, Berner H, Berger ML, Wolschann P (2013) Holographic quantitative structure-activity relationships of tryptamine derivatives at NMDA, $5HT_{1A}$ and $5HT_{2A}$ receptors. Molecules 18 (8):8799–8811
154. Muñoz-Gutiérrez C, Caballero J, Morales-Bayuelo A (2016) HQSAR and molecular docking studies of furanyl derivatives as adenosine A_{2A} receptor antagonists. Med Chem Res 25(7):1316–1328
155. Doytchinova I (2001) CoMFA-based comparison of two models of binding site on adenosine A_1 receptor. J Comput Aided Mol Des 15(1):29–39
156. Lima E, Teixeira-Salmela LF, Simoes L, Guerra AC, Lemos A (2016) Assessment of the measurement properties of the post stroke motor function instruments available in Brazil: a systematic review. Braz J Phys Ther 20 (2):114–125
157. Pourbasheer E, Shokouhi Tabar S, Masand V, Aalizadeh R, Ganjali M (2015) 3D-QSAR and docking studies on adenosine A_{2A} receptor antagonists by the CoMFA method. SAR QSAR Environ Res 26(6):461–477
158. Rieger JM, Brown ML, Sullivan GW, Linden J, Macdonald TL (2001) Design, synthesis, and evaluation of novel A_{2A} adenosine receptor agonists. J Med Chem 44(4):531–539
159. Baraldi PG, Borea PA, Bergonzoni M, Cacciari B, Ongini E, Recanatini M, Spalluto G (1999) Comparative molecular field analysis (CoMFA) of a series of selective adenosine receptor A_{2A} antagonists. Drug. Dev Res 46 (2):126–133
160. Doytchinova I, Valkova I, Natcheva R (2001) CoMFA study on adenosine A_{2A} receptor agonists. Quant Struct-Act Relat 20 (2):124–129
161. Vilar S, Karpiak J, Costanzi S (2010) Ligand and structure-based models for the prediction of ligand-receptor affinities and virtual screenings: development and application to the β_2-adrenergic receptor. J Comput Chem 31 (4):707–720
162. Senthil Kumar P, Bharatam PV (2010) Comparative 3D QSAR study on β_1-, β_2-, and β_3-adrenoceptor agonists. Med Chem Res 19 (9):1121–1140
163. Jozwiak K, Khalid C, Tanga MJ, Berzetei-Gurske I, Jimenez L, Kozocas JA, Woo A, Zhu W, Xiao RP, Abernethy DR, Wainer IW (2007) Comparative molecular field analysis of the binding of the stereoisomers of fenoterol and fenoterol derivatives to the β_2 adrenergic receptor. J Med Chem 50 (12):2903–2915
164. Jozwiak K, Woo AY, Tanga MJ, Toll L, Jimenez L, Kozocas JA, Plazinska A, Xiao RP, Wainer IW (2010) Comparative molecular field analysis of fenoterol derivatives: a platform towards highly selective and effective β_2-adrenergic receptor agonists. Bioorg Med Chem 18(2):728–736
165. Plazinska A, Pajak K, Rutkowska E, Jimenez L, Kozocas J, Koolpe G, Tanga M, TollL WIW, Jozwiak K (2014) Comparative molecular field analysis of fenoterol derivatives interacting with an agonist-stabilized form of the β_2-adrenergic receptor. Bioorg Med Chem 22(1):234–246
166. Gunda SK, Anugolu RK, Tata SR, Mahmood S (2012) Structural investigations of $CXCR_2$ receptor antagonists by CoMFA, CoMSIA and flexible docking studies. Acta Pharma 62 (3):287–304
167. Peng Y, Keenan SM, Zhang Q, Welsh WJ (2005) 3D-QSAR comparative molecular field analysis on δ opioid receptor agonist SNC80 and its analogs. J Mol Graph Model 24(1):25–33
168. Ghasemi JB, Tavakoli H (2012) Improvement of the prediction power of the CoMFA and CoMSIA models on histamine H_3 antagonists by different variable selection methods. Sci Pharm 80(3):547–566
169. Chen HF (2008) Computational study of histamine H_3-receptor antagonist with support vector machines and three dimension quantitative structure activity relationship methods. Anal Chim Acta 624(2):203–209
170. Rivara S, Mor M, Bordi F, Silva C, Zuliani V, Vacondio F, Morini G, Plazzi P, Carrupt PA, Testa B (2003) Synthesis and three-dimensional quantitative structure-activity relationship analysis of H_3 receptor antagonists containing a neutral heterocyclic polar group. Drug Des Discov 18(2–3):65–79
171. Sekhar YN, Ravikumar M, Nayana MRS, Mallena SC, Kumar MK (2008) 3D-QSAR studies of triazafluorenone inhibitors of metabotropic glutamate receptor subtype 1. Eur J Med Chem 43(5):1025–1034
172. Sekhar YN, Nayana MRS, Ravikumar M, Mahmood S (2007) Comparative molecular field analysis of quinoline derivatives as

selective and noncompetitive $mGluR_1$ antagonists. Chem Biol Drug Des 70 (6):511–519

173. Tresadern G, Cid JM, Trabanco AA (2014) QSAR design of triazolopyridine $mGlu_2$ receptor positive allosteric modulators. J Mol Graph Model 53:82–91
174. de Paulis T, Hemstapat K, Chen Y, Zhang Y, Saleh S, Alagille D, Baldwin RM, Tamagnan GD, Conn PJ (2006) Substituent effects of *N*-(1,3-Diphenyl-1*H*-pyrazol-5-yl)benzamides on positive allosteric modulation of the metabotropic glutamate-5 receptor in rat cortical astrocytes. J Med Chem 49 (11):3332–3344
175. Lowe JEW, Ferrebee A, Rodriguez AL, Conn PJ, Meiler J (2010) 3D-QSAR CoMFA study of benzoxazepine derivatives as $mGluR_5$ positive allosteric modulators. Bioorg Med Chem Lett 20(19):5922–5924
176. Selvam C, Thilagavathi R, Narasimhan B, Kumar P, Jordan BC, Ranganna K (2016) Computer-aided design of negative allosteric modulators of metabotropic glutamate receptor 5 ($mGluR_5$): comparative molecular field analysis of aryl ether derivatives. Bioorg Med Chem Lett 26(4):1140–1144
177. Zlotos DP, Buller S, Stiefl N, Baumann K, Mohr K (2004) Probing the pharmacophore for allosteric ligands of muscarinic M_2 receptors: SAR and QSAR studies in a series of bisquaternary salts of caracurine V and related ring systems. J Med Chem 47 (14):3561–3571
178. Niu YY, Yang LM, Deng KM, Yao JH, Zhu L, Chen CY, Zhang M, Zhou JE, Shen TX, Chen HZ (2007) Quantitative structure–-selectivity relationship for M_2 selectivity between M_1 and M_2 of piperidinyl piperidine derivatives as muscarinic antagonists. Bioorg Med Chem Lett 17(8):2260–2266
179. Silva ME, Heim R, Strasser A, Elz S, Dove S (2011) Theoretical studies on the interaction of partial agonists with the 5-HT_{2A} receptor. J Comput Aided Mol Des 25(1):51–66
180. Moeller D, Salama I, Kling RC, Hübner H, Gmeiner P (2015) 1,4-Disubstituted aromatic piperazines with high 5-HT_{2A}/D_2 selectivity: quantitative structure-selectivity investigations, docking, synthesis and biological evaluation. Bioorg Med Chem 23 (18):6195–6209
181. Raviña E, Negreira J, Cid J, Masaguer CF, Rosa E, Rivas ME, Fontenla JA, Loza MI, Tristán H, Cadavid MI, Sanz F, Lozoya E, Carotti A, Carrieri A (1999) Conformationally constrained butyrophenones with mixed dopaminergic (D_2) and serotoninergic (5-HT_{2A}, 5-HT_{2C}) affinities: synthesis, pharmacology, 3D-QSAR, and molecular modeling of (aminoalkyl)benzo- and -thienocycloalkanones as putative atypical antipsychotics. J Med Chem 42(15):2774–2797
182. Zhang Z, An L, Hu W, Xiang Y (2007) 3D-QSAR study of hallucinogenic phenylalkylamines by using CoMFA approach. J Comput Aided Mol Des 21(4):145–153
183. Bromidge SM, Dabbs S, Davies DT, Duckworth DM, Forbes IT, Ham P, Jones GE, King FD, Saunders DV, Starr S, Thewlis KM, Wyman PA, Blaney FE, Naylor CB, Bailey F, Blackburn TP, Holland V, Kennett GJ, Riley GJ, Wood MD (1998) Novel and selective 5-$HT_{2C/2B}$ receptor antagonists as potential anxiolytic agents: synthesis, quantitative structure–activity relationships, and molecular modeling of substituted 1-(3-pyridylcarbamoyl)indolines. J Med Chem 41 (10):1598–1612
184. Lopez-Rodriguez ML, Murcia M, Benhamú B, Viso A, Campillo M, Pardo L (2001) 3D-QSAR/CoMFA and recognition models of benzimidazole derivatives at the 5-HT_4 receptor. Bioorg Med Chem Lett 11 (21):2807–2811
185. López-Rodríguez ML, Murcia M, Benhamú B, Viso A, Campillo M, Pardo L (2002) Benzimidazole derivatives. 3. 3D-QSAR/CoMFA model and computational simulation for the recognition of 5-HT_4 receptor antagonists. J Med Chem 45(22):4806–4815
186. Iskander MN, Leung LM, Buley T, Ayad F, Di Iulio J, Tan YY, Coupar IM (2006) Optimization of a pharmacophore model for 5-HT_4 agonists using CoMFA and receptor based alignment. Eur J Med Chem 41 (1):16–26
187. Suzuki T, Imanishi N, Itahana H, Watanuki S, Miyata K, Ohta M, Nakahara H, Yamagiwa Y, Mase T (1998) Novel 5-hydroxytryptamine 4 (5-HT_4) receptor agonists. Synthesis and Gastroprokinetic activity of 4-amino-*N* (2-(1-aminocycloalkan-1-yl) ethyl)-5-chloro-2 methoxybenzamides. Chem Pharm Bull 46 (7):1116–1124
188. Doddareddy MR, Cho YS, Koh HY, Pae AN (2004) CoMFA and CoMSIA 3D QSAR analysis on N_1-arylsulfonylindole compounds as 5-HT_6 antagonists. Bioorg Med Chem 12 (15):3977–3985
189. Guner OF (2005) The impact of pharmacophore modeling in drug design. IDrugs 8 (7):567–572
190. Sun H (2008) Pharmacophore-based virtual screening. Curr Med Chem 15 (10):1018–1024

191. Dixon SL, Smondyrev AM, Knoll EH, Rao SN, Shaw DE, Friesner RA (2006) PHASE: a new engine for pharmacophore perception, 3D QSAR model development, and 3D database screening: 1. Methodology and preliminary results. J Comput Aided Mol Des 20 (10–11):647–671
192. Golender V, Vesterman B, Eliyahu O, Kardash A, Kletzin M, Shokhen M, Vorpagel E (1994) Knowledge engineering approach to drug design and its implementation in the APEX-3D Expert System. In: Proceedings of the 10th European Symposium on Structure-Activity Relationships, Barcelona: Prous Science, pp 249–254
193. Harris DL, Loew G (2008) Development and assessment of a 3D pharmacophore for ligand recognition of BDZR/GABAA receptors initiating the anxiolytic response. Bioorg Med Chem 8(11):2527–2538
194. Mills JEJ, de Esch IJP, Perkins TDJ, Dean PM (2001) SLATE: a method for the superposition of flexible ligands. J Comput Aided Mol Des 15(1):81–96
195. Wolber G, Langer T (2005) LigandScout: 3-D pharmacophores derived from protein-bound ligands and their use as virtual screening filters. J Chem Inf Model 45(1):160–169
196. Huang P, Kim S, Loew G (1997) Development of a common 3D pharmacophore for δ-opioid recognition from peptides and non-peptides using a novel computer program. J Comput Aided Mol Des 11(1):21–28
197. Clark M, Cramer RD, Van Opdenbosch N (1989) Validation of the general purpose Tripos 5.2 force field. J Comput Chem 10 (8):982–1012
198. Patel Y, Gillet VJ, Bravi G, Leach AR (2002) A comparison of the pharmacophore identification programs: CATALYST, DISCO and GASP. J Comput Aided Mol Des 16 (8–9):653–681
199. Chen IJ, Foloppe N (2008) Conformational sampling of druglike molecules with MOE and CATALYST: implications for pharmacophore modeling and virtual screening. J Chem Inf Model 48(9):1773–1791
200. Mustyala KK, Chitturi AR, Naikal James PS, Vuruputuri U (2012) Pharmacophore mapping and in silico screening to identify new potent leads for A_{2A} adenosine receptor as antagonists. J Recept Signal Transduct Res 32(2):102–113
201. Bacilieri M, Ciancetta A, Paoletta S, Federico S, Cosconati S, Cacciari B, Taliani S, Da Settimo F, Novellino E, Klotz KN, Spalluto G, Moro S (2013) Revisiting a receptor-based pharmacophore hypothesis for human A_{2A} adenosine receptor antagonists. J Chem Inf Model 53(7):1620–1637
202. Wei J, Wang S, Gao S, Dai X, Gao Q (2007) 3D-Pharmacophore models for selective A_{2A} and A_{2B} adenosine receptor antagonists. J Chem Inf Model 47(2):613–625
203. Khanfar MA, Al-Qtaishat S, Habash M, Taha MO (2016) Discovery of potent adenosine A_{2A} antagonists as potential anti-Parkinson disease agents. Non-linear QSAR analyses integrated with pharmacophore modeling. Chem Biol Interact 254:93–101
204. Balogh B, Jójárt B, Wágner Z, Kovács P, Máté G, Gyires K, Zádori Z, Falkay G, Márki Á, Viskolcz B, Mátyus P (2007) 3D QSAR models for α_{2A}-adrenoceptor agonists. Neurochem Int 51(5):268–276
205. Kothandan G, Gadhe CG, Madhavan T, Cho SJ (2011) Binding site analysis of CCR_2 through in silico methodologies: docking, CoMFA, and CoMSIA. Chem Biol Drug Des 78(1):161–174
206. Singh R, Balupuri A, Sobhia ME (2013) Development of 3D-pharmacophore model followed by successive virtual screening, molecular docking and ADME studies for the design of potent CCR_2 antagonists for inflammation-driven diseases. Mol Simul 39 (1):49–58
207. Ye Y, Liao Q, Wei J, Gao Q (2010) 3D-QSAR study of corticotropin-releasing factor 1 antagonists and pharmacophore-based drug design. Neurochem Int 56(5):107–117
208. Whitten JP, Xie YF, Erickson PE, Webb TR, De Souza EB, Grigoriadis DE, McCarthy JR (1996) Rapid microscale synthesis, a new method for lead optimization using robotics and solution phase chemistry: application to the synthesis and optimization of corticotropin-releasing factor 1 receptor antagonists. J Med Chem 39(22):4354–4357
209. Kaur P, Sharma V, Kumar V (2012) pharmacophore modelling and 3D-QSAR studies on N^3-phenylpyrazinones as corticotropin-releasing factor 1 receptor antagonists. Int J Med Chem 2012:452325. doi:10.1155/2012/452325
210. Bernard D, Coop A, MacKerell AD (2003) 2D conformationally sampled pharmacophore: a ligand-based pharmacophore to differentiate δ opioid agonists from antagonists. J Am Chem Soc 125(10):3101–3107
211. Coop A, Jacobson AE (1999) The LMC δ opioid recognition pharmacophore: comparison of SNC80 and oxymorphindole. Bioorg Med Chem Lett 9(3):357–362

212. Bernard D, Coop A, MacKerell AD (2005) Conformationally sampled pharmacophore for peptidic δ opioid ligands. J Med Chem 48(24):7773–7780
213. Levoin N, Labeeuw O, Krief S, Calmels T, Poupardin-Olivier O, Berrebi-Bertrand I, Lecomte JM, Schwartz JC, Capet M (2013) Determination of the binding mode and interacting amino-acids for dibasic H_3 receptor antagonists. Bioorg Med Chem 21 (15):4526–4529
214. De Esch IJP, Mills JEJ, Perkins TDJ, Romeo G, Hoffmann M, Wieland K, Leurs R, WMPB M, PHJ N, Dean PM, Timmerman H (2001) Development of a pharmacophore model for histamine H_3 receptor antagonists, using the newly developed molecular modeling program SLATE. J Med Chem 44 (11):1666–1674
215. Axe FU, Bembenek SD, Szalma S (2006) Three-dimensional models of histamine H_3 receptor antagonist complexes and their pharmacophore. J Mol Graph Model 24 (6):456–464
216. Jullian N, Brabet I, Pin JP, Acher FC (1999) Agonist selectivity of $mGluR_1$ and $mGluR_2$ metabotropic receptors: a different environment but similar recognition of an extended glutamate conformation. J Med Chem 42 (9):1546–1555
217. Filizola M, Tasso SM, Loew GH, Villar HO (2001) Global physicochemical properties as activity discriminants for the $mGluR_1$ subtype of metabotropic glutamate receptors. J Comput Chem 22(16):2018–2027
218. Zhang MQ, Zhang XL, Li Y, Fan WJ, Wang YH, Hao M, Zhang SW, Ai CZ (2011) Investigation on quantitative structure activity relationships and pharmacophore modeling of a series of $mGluR_2$ antagonists. Int J Mol Sci 12 (9):5999–6023
219. Lu C, Jin F, Li C, Li W, Liu G, Tang Y (2011) Insights into binding modes of 5-HT_{2C} receptor antagonists with ligand-based and receptor-based methods. J Mol Model 17 (10):2513–2523
220. Ahmed A, Choo H, Cho YS, Park WK, Pae AN (2009) Identification of novel serotonin 2C receptor ligands by sequential virtual screening. Bioorg Med Chem 17 (13):4559–4568
221. Iskander MN, Coupar IM, Winkler DA (1999) Investigation of 5-HT_4 agonist activities using molecular field analysis. J Chem Soc Perkin Trans 2(2):153–158
222. Bureau R, Daveu C, Lemaître S, Dauphin F, Landelle H, Lancelot JC, Rault S (2002) Molecular design based on 3D-pharmacophore. Application to 5-HT_4 receptor. J Chem Inf Comput Sci 42(4):962–967
223. López-Rodríguez ML, Benhamú B, de la Fuente T, Sanz A, Pardo L, Campillo M (2005) A three-dimensional pharmacophore model for 5-hydroxytryptamine 6 (5-HT_6) receptor antagonists. J Med Chem 48 (13):4216–4219
224. Kim HJ, Doddareddy MR, Choo H, Cho YS, No KT, Park WK, Pae AN (2008) New serotonin 5-HT_6 ligands from common feature pharmacophore hypotheses. J Chem Inf Model 48(1):197–206
225. Hayat F, Cho S, Rhim H, Indu Viswanath AN, Pae AN, Lee JY, Choo DJ, Choo HY (2013) Design and synthesis of novel series of 5-HT_6 receptor ligands having indole, a central aromatic core and 1-amino-4-methyl piperazine as a positive ionizable group. Bioorg Med Chem 21(17):5573–5582